Research paper

Anisotropic evolution of viscous strain in soft biological materials

Jacopo Ciambella, Giulio Lucci *, Paola Nardinocchi

Department of Structural and Geotechnical Engineering, Sapienza Università di Roma, Via Eudossiana 18, Rome, 00184, Italy

ARTICLE INFO

ABSTRACT

We propose a model for anisotropic viscoelastic biological materials that can handle large deformations, based on the kinematic assumption that the reinforcing fibre structure undergoes affine deformation with the underlying matrix. A generalized orientation tensor approach is used to account for the dispersion of the fibres. Moreover, we consider a strain energy function that features both an elastic and an overstress component, corresponding to distinct natural states. As a consequence of this choice, the remodelled state is not necessarily stress-free, and the material does not completely relax the stress. Notably, we consider that viscous remodelling also alters the fibre distribution, leading to a dependence of the overstress energy on the remodelled orientation tensor. An anisotropic evolution equation for the viscous strain is then derived, which has five distinct characteristic times if a single fibre family is considered and requires no additional assumptions on the viscous spin. To implement the model, we prove that the evolution of the viscous strain can be recast in a variational form by an Onsager variational principle. Finally, we discuss the algorithm used for the simulations and show numerical examples that serve as benchmark test cases for viscoelastic materials.

1. Introduction

Biological tissues exhibit viscoelastic behaviour which manifests as a combination of solid-like and fluid-like properties contingent on applied force and time scale (Fung, 1993). Viscoelasticity in biological tissues may indeed serve as a crucial biomarker, reflecting the structural and functional alterations in tissues under diverse health and disease conditions (Mierke, 2022). Consequently, the comprehension and measurement of viscoelastic properties in biological tissues stand as essential pursuits in biomechanics research and biomedical applications (Gotschi et al., 2023).

Soft biological tissues are usually treated as nearly incompressible materials due to their high water content. Comprising an isotropic soft matrix (mainly elastin) and stiffer collagen fibres, these tissues exhibit fibre orientation and dispersion patterns specific to the tissue type and body location (Canham et al., 1989; Komai and Ushiki, 1991; Finlay et al., 1998; Boote et al., 2006; Schriefl et al., 2011).

In particular, there are two main methods for modelling reinforced soft tissues. The first method treats matrix and fibres as separate entities (Lanir, 1979) and uses appropriate kinematic assumptions and a rule of mixture to derive the overall tissue response (Lanir, 2017). The second method instead views matrix and fibres as a single homogenized continuum, whose anisotropic material response reflects fibre distribution (Fung, 1993; Latorre and Montáns, 2016; Grillo et al., 2014; Hashlamoun et al., 2016).

Among the continuum models, the angular integration approach (Sacks, 2003; Driessen et al., 2005; Ateshian et al., 2009) computes the fibre orientation distribution at every integration point, resulting in a computationally expensive numerical procedure. In contrast, generalized structure tensor (GST) models preprocess the fibre orientation distribution and represent it using tensors that encapsulate distribution moments (Freed et al., 2005; Gasser et al., 2006; Pandolfi and Vasta, 2012a,b; Wollner et al., 2023). While GST models lack the ability to differentiate between fibres under varying deformation states, they offer superior computational efficiency (Verron, 2015). This type of models proved to be efficient to describe soft biological tissues with distributed fibres and their material response (Gizzi et al., 2016b; Pandolfi et al., 2017, 2016; Pandolfi and Vasta, 2012b; Teichtmeister and Holzapfel, 2022).

Concerning the modelling of viscous effects, a continuum approach to model the viscoelasticity of soft tissues at large strain builds on the extension of simple rheological models, such as the Maxwell model, the Kelvin model, and the generalized Maxwell model, to finite deformations (Reese and Govindjee, 1998; Upadhyay et al., 2020; Coco and Saccomandi, 2023). This is typically accomplished by assuming a multiplicative decomposition of the deformation gradient or an additive decomposition of the Cauchy stress into elastic and viscous components. In this framework, Latorre and Montáns (2015, 2016) introduced a remodelled state of the continuum and an anisotropic strain energy density solely dependent on the elastic component of the deformation,

* Corresponding author.

E-mail address: giulio.lucci@uniroma1.it (G. Lucci).

which plays the role of an internal-like variable whose evolution is governed by a kinetic equation. Similarly, Liu et al. (2019) assumed that the amount of elastic deformation experienced by the matrix and fibres differs, leading to a separate multiplicative decomposition for each component.

In a recent development, Sadik and Yavari (2024) introduced a geometric perspective on the multiplicative decomposition of the deformation gradient. They highlighted the crucial distinction that viscoelastic materials, unlike traditional inelastic solids, do not relax to a zero-stress state. To accommodate this behaviour, they used an additive decomposition of the elastic strain energy density into two components: one dependent on the elastic part of the deformation gradient and the other on the complete deformation gradient, a concept also used in Reese and Govindjee (1998), Latorre and Montáns (2015) and Liu et al. (2019). Notably, both components of the strain energy share the same material symmetry, defined by the reference orientation of the fibres.

A different approach was instead introduced in Ciambella and Nardinocchi (2021), based on a novel anisotropic inelastic model that accounts for fibre remodelling during viscous deformation. The consequent evolution of the material symmetry from the reference configuration to the natural state was also included in the constitutive theory, which was also required to be structurally frame indifferent (SFI).

Here, we build upon the work in Ciambella and Nardinocchi (2021) and propose a wider model that incorporates several key features. First, the viscous component of the deformation gradient is explicitly linked to the remodelling of the fibre structure, which, in turn, affects the material's anisotropic behaviour. Secondly, fibre dispersion is accounted for using a generalized orientation tensor approach. Thirdly, the model allows for the presence of an overstress, which makes the remodelled state not necessarily stress-free.

These assumptions lead to a dynamical evolution of the viscous stretch, governed by five characteristic times for a single fibre family. Specifically, the proposed constitutive model exhibits a material behaviour that transitions from anisotropic hyperelasticity at high deformation rates to anisotropic Ericksen fluid behaviour at low deformation rates.

In detail, the paper is organized as follows. In Section 2 we present the kinematics of the model and discuss how the fibre distribution is accounted for. Section 3 describes the energetic choices and derives thermodynamically consistent constitutive equations. Then, through a careful analysis, in Section 4 we demonstrate that the flow rule can be reformulated in referential terms, without the need of imposing any additional constraints on the viscous spin rate, and it can be recast in a variational form through an Onsager variational principle. Several examples that showcase the capabilities of the model are presented in Section 5, allowing to compare its outcomes against benchmark test cases for viscoelastic materials. Finally, in Section 6 we provide some concluding remarks and discuss future perspectives.

2. Kinematics and reoriented fibre distribution

We identify the material body with its reference configuration Ω, which is a regular region of the three-dimensional Euclidean space $\mathcal{E}$, and denote with $X \in \Omega$ the generic material point. The deformation map $\chi : \Omega \times \mathcal{I} \to \mathcal{E}$ assigns to each point $X \in \Omega$ at any time $t \in \mathcal{I}$ a position $x = \chi(X, t) \in \mathcal{E}$. The image of the map at the current time identifies the current configuration Ω_t, which represents the deformed state of the material body. The deformation gradient $\mathbf{F} = \nabla \chi$ quantifies the local alteration in both length and orientation of material line elements due to the deformation χ.

The macroscopic deformation gradient $\mathbf{F}$ is multiplicatively decomposed (Lee, 1969) into an elastic $\mathbf{F}_e$ and a viscous $\mathbf{F}_v$ component and expressed as:

$$\mathbf{F} = \mathbf{F}_e \mathbf{F}_v \quad \text{with} \quad J_e = \det \mathbf{F}_e > 0 \quad \text{and} \quad J_v = \det \mathbf{F}_v > 0. \quad (2.1)$$

As a consequence, $J = \det \mathbf{F} = J_e J_v$. The decomposition (2.1), sketched in Fig. 1a, provides an understanding of the interplay between elastic and viscous components in producing the macroscopic deformation.

The fibre dispersion in the reference configuration is accounted for by introducing the reference *generalized orientation tensor*[1]

$$\mathbf{A}_0 = \int_S \rho(\mathbf{m}) \, \mathbf{m} \otimes \mathbf{m} \, d\mathbf{m}, \qquad \text{s.t.} \quad \int_S \rho(\mathbf{m}) = 1, \quad \text{and} \quad |\mathbf{m}| = 1, \quad (2.2)$$

in which the fibre-related probability density function ρ satisfies the normalization condition when computed over the unit sphere S. So, the generalized orientation tensor possesses the normalization property $\mathbf{I} \cdot \mathbf{A}_0 = 1$, where $\mathbf{I}$ is the identity tensor and $\cdot$ denotes the inner product between tensors. We remark that $\mathbf{A}_0$, which is a symmetric positive semi-definite tensor, represents the second moment of the probability distribution $\rho(\mathbf{m})$. On assuming that fibres deform as material line elements[2] and that the viscous component $\mathbf{F}_v$ of the deformation corresponds to a remodelled state, the generalized orientation tensor in the remodelled state is defined as follows:

$$\mathbf{A}_v = \frac{\mathbf{F}_v \mathbf{A}_0 \mathbf{F}_v^{\mathrm{T}}}{\mathbf{I} \cdot \mathbf{F}_v \mathbf{A}_0 \mathbf{F}_v^{\mathrm{T}}} \qquad \text{with} \quad \mathbf{I} \cdot \mathbf{A}_v = 1, \quad (2.3)$$

whereas the orientation tensor in the current state is (see Fig. 1a):

$$\mathbf{A} = \frac{\mathbf{F}_e \mathbf{A}_v \mathbf{F}_e^{\mathrm{T}}}{\mathbf{I} \cdot \mathbf{F}_e \mathbf{A}_v \mathbf{F}_e^{\mathrm{T}}} \qquad \text{with} \quad \mathbf{I} \cdot \mathbf{A} = 1.$$

The multiplicative decomposition of the deformation gradient (2.1) brings into the model different strain measures, namely the visible right Cauchy–Green strain $\mathbf{C}$ and its viscous $\mathbf{C}_v$ and elastic $\mathbf{C}_e$ counterparts:

$$\mathbf{C} = \mathbf{F}^{\mathrm{T}}\mathbf{F}, \qquad \mathbf{C}_v = \mathbf{F}_v^{\mathrm{T}}\mathbf{F}_v, \qquad \mathbf{C}_e = \mathbf{F}_e^{\mathrm{T}}\mathbf{F}_e = \mathbf{F}_v^{-\mathrm{T}}\mathbf{C}\mathbf{F}_v^{-1}. \quad (2.4)$$

Eq. (2.4)$_3$ shows that the elastic strain $\mathbf{C}_e$ can be represented in terms of the viscous deformation $\mathbf{F}_v$ and the current strain $\mathbf{C}$. Based on the previous kinematic assumptions, the viscous deformation rate tensor is

$$\mathbf{L}_v = \dot{\mathbf{F}}_v \mathbf{F}_v^{-1}, \quad (2.5)$$

that can be additively decomposed into the viscous stretch rate $\mathbf{D}_v = \mathrm{sym}\,\mathbf{L}_v$ and the viscous spin $\mathbf{W}_v = \mathrm{skw}\,\mathbf{L}_v$. The following kinematic relations arise as well:

$$\dot{\mathbf{C}} = 2\mathbf{F}^{\mathrm{T}}\mathbf{D}\mathbf{F}, \quad (2.6)$$

$$\dot{\mathbf{C}}_e = 2\mathbf{F}_e^{\mathrm{T}}\mathbf{D}\mathbf{F}_e - \mathbf{C}_e\mathbf{L}_v - \mathbf{L}_v^{\mathrm{T}}\mathbf{C}_e, \quad (2.7)$$

$$\dot{\mathbf{A}}_v = \mathbf{L}_v\mathbf{A}_v + \mathbf{A}_v\mathbf{L}_v^{\mathrm{T}} - 2(\mathbf{A}_v \cdot \mathbf{D}_v)\mathbf{A}_v, \quad (2.8)$$

where $\mathbf{D} = \mathrm{sym}\,(\dot{\mathbf{F}}\mathbf{F}^{-1})$ is the stretch rate. It is noteworthy that Eq. (2.8) ensures that $\mathbf{A}_v$ maintains a trace of 1 throughout its evolution.

Remark 1. When the fibre dispersion is planar, there is a one-to-one mapping between the unit tensor $\mathbf{A}_0$ and the angle θ that the fibre forms with a reference axis $\mathbf{e}_1$. Then, the definition of $\mathbf{A}_0$ in (2.2) simplifies as:

$$\mathbf{A}_0 = \pi \int_{-\pi/2}^{\pi/2} \rho(\theta) \, \mathbf{m}(\theta) \otimes \mathbf{m}(\theta) \, d\theta. \quad (2.9)$$

In addition, if the dispersed fibres are symmetrically distributed around a mean direction $\mathbf{a}_0$, that is, $\rho(\theta) = \rho(-\theta) \; \forall \theta$, then the following is obtained in terms of the dispersion parameter $\kappa \in [0, 1/2]$ (Teichtmeister and Holzapfel, 2022):

$$\mathbf{A}_0 = \kappa \mathbf{I} + (1 - 2\kappa)\mathbf{a}_0 \otimes \mathbf{a}_0, \qquad \text{with} \quad \kappa = \pi \int_{-\pi/2}^{\pi/2} \rho(\theta) \sin^2 \theta \, d\theta,$$

---

[1] It is also referred to as generalized structure tensor (Gasser et al., 2006; Gizzi et al., 2016a; Pandolfi and Vasta, 2012b).

[2] A possible modelling alternative consists in assuming non-affine remodelling of the fibre structure, which renders remodelling of material line elements different from remodelling of fibres, see for instance (Ciambella and Nardinocchi, 2019, 2022; Ciambella et al., 2022).
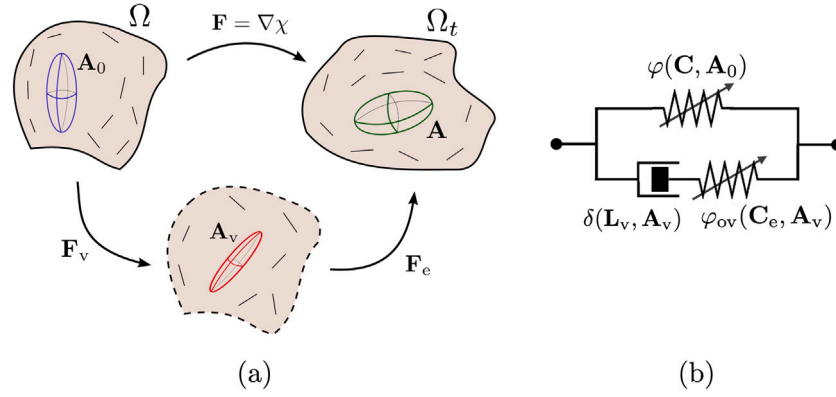
Fig. 1. (a): Multiplicative decomposition of the deformation gradient: $\mathbf{A}_0$, $\mathbf{A}_v$, and $\mathbf{A}$ are the generalized orientation tensors in the reference, remodelled, and current states, respectively. (b): Rheological model corresponding to the energy choice of Eq. (3.11). The arrows on the springs are used to highlight the fact that the elastic behaviour, represented by φ and φ_{ov}, is anisotropic. Here, φ corresponds to the specific elastic energy associated with the visible strain $\mathbf{C}$ and reference orientation tensor $\mathbf{A}_0$, while φ_{ov} is the specific elastic energy linked to the elastic strain $\mathbf{C}_e$ and remodelled generalized orientation tensor $\mathbf{A}_v$. Additionally, δ represents the specific dissipation density corresponding to the damper.

We also notice that the case of a standard transversely isotropic material, in which a single preferential direction $\mathbf{a}_0$ exists, is recovered as a particular case on assuming that the probability distribution is a Dirac delta centred in $\mathbf{a}_0$, i.e., $\rho(\mathbf{m}) = \delta_{\mathbf{a}_0}(\mathbf{m})$. In such a case, $\mathbf{A}_0 = \mathbf{a}_0 \otimes \mathbf{a}_0$.

In this limiting case, the orientation tensor in the remodelled state (2.3) simplifies into

$$\mathbf{A}_v = \mathbf{a}_v \otimes \mathbf{a}_v, \qquad \mathbf{a}_v = \frac{\mathbf{F}_v \mathbf{a}_0}{|\mathbf{F}_v \mathbf{a}_0|}, \tag{2.10}$$

which is coherent with the remodelling framework introduced in Ciambella and Nardinocchi (2021).

Remark 2. The consideration of multiple fibre distributions can be achieved by assuming the existence of additional mean orientations in the reference configuration, denoted as $\mathbf{a}_0^i$, $i = 1, \ldots, M$. Consequently, multiple generalized orientation tensors $\mathbf{A}_0^i$ would be introduced, each one associated with its respective distribution ρ^i. While the incorporation of these tensors into the current model is straightforward, for the sake of clarity, we will not delve into it in this context.

3. Energies, stresses, and remodelling action

In remodelling theories, the multiplicative decomposition is inherently tied to constitutive information. The non-elastic part of the deformation gradient is not merely a kinematic descriptor of remodelling in an underlying intermediate state, but it carries constitutive information in the observed current state where actual displacements occur (DiCarlo and Quiligotti, 2002). Typically, it characterizes the intermediate state as stress-free with zero elastic energy, which justifies the usual definition of the intermediate state as the *natural state*. Consequently, the evolution of $\mathbf{F}_v$ is usually assumed to govern the evolution of the stress-free state of the body.

Here, we adopt a different perspective and consider the possibility that the intermediate state is not stress-free. Stresses arise from the deformation gradient even when $\mathbf{F}_e = \mathbf{I}$, while overstresses are driven by an elastic component of the deformation $\mathbf{F}_e \neq \mathbf{I}$. This viewpoint aligns with the rheological model depicted in Fig. 1b and is consistent with various approaches in the literature, where overstresses are sometimes referred to as non-equilibrium stresses[3] (Reese and Govindjee, 1998; Sadik and Yavari, 2024).

3.1. Elastic energies

We assume that the elastic energy ϕ per unit mass,[4] referred to hereafter as the specific elastic energy, comprises two components: the overstress φ_{ov} and the elastic φ components. The two components correspond to distinct natural states and are meant to describe the viscoelastic behaviour of the material; in this sense, they encompass the elasticity of the springs in Fig. 1b.

We posit that $\varphi_{ov} = \hat{\varphi}_{ov}(\mathbf{C}_e, \mathbf{A}_v)$ depends on the elastic strain $\mathbf{C}_e$ and on the remodelled generalized orientation tensor $\mathbf{A}_v$ in such a way that, for all $\mathbf{A}_v$, $\hat{\varphi}_{ov}(\mathbf{I}, \mathbf{A}_v) = 0$. On the other side, we assume that $\varphi = \hat{\varphi}(\mathbf{C}, \mathbf{A}_0)$ depends on the current strain $\mathbf{C}$ and the reference generalized orientation tensor $\mathbf{A}_0$ in such a way that, for all $\mathbf{A}_0$, $\hat{\varphi}(\mathbf{I}, \mathbf{A}_0) = 0$.

As a consequence, the specific energy density is represented as

$$\phi = \hat{\phi}(\mathbf{C}, \mathbf{C}_e, \mathbf{A}_0, \mathbf{A}_v) = \hat{\varphi}_{ov}(\mathbf{C}_e, \mathbf{A}_v) + \hat{\varphi}(\mathbf{C}, \mathbf{A}_0). \tag{3.11}$$

Eq. (3.11) and the considerations outlined above reveal several key points: (i) the reference state is a natural state for the specific energy φ; (ii) the remodelled state, where $\mathbf{F}_e = \mathbf{I}$, is a natural state for φ_{ov}; (iii) the remodelled state is not necessarily stress-free, owing to the energetic component φ.

It is worth noting that the overstress energy φ_{ov} is contingent on the remodelled generalized orientation tensor $\mathbf{A}_v$, which represents the fibre distribution in the natural state for φ_{ov}. This distinction marks a notable aspect of our approach, setting it apart from other recent proposals where any consideration on the remodelled anisotropic structure is absent (Sadik and Yavari, 2024).

Let us also note that the function φ_{ov} is structurally frame indifferent. SFI was originally introduced by Green and Naghdi (1971) to filter out the rotation indeterminacy associated with the multiplicative decomposition from the constitutive model. Subsequently, it was established that for a strain energy function solely dependent on the elastic strain $\mathbf{C}_e$, SFI implies isotropy of the material (Gurtin et al., 2013). In this paper, where the strain energy density depends both on $\mathbf{C}_e$ and $\mathbf{A}_v$, SFI equates to imposing transverse isotropy in the remodelled state, as demonstrated in Ciambella and Nardinocchi (2021).

Remark 3. In the literature, the energy densities φ and φ_{ov} are often labelled as the equilibrium and non-equilibrium components, denoted as φ_{Eq} and φ_{NEq}, respectively (Reese and Govindjee, 1998; Sadik and

---

[3] This point of view differs from that introduced in Ciambella and Nardinocchi (2021). Therein, with the aim to recover the anisotropic Ericksen fluid material behaviour, only the contribution of the elastic deformation to the stress was accounted for and the intermediate state was indeed a natural state.

[4] The theory is developed assuming mass conservation, which leads to the relationships $\varrho_0 = J\varrho = J_v\varrho_v$ among the mass densities ϱ_0, ϱ_v, and ϱ per unit reference, remodelled, and current volume, respectively.

Yavari, 2024; Kumar and Lopez-Pamies, 2016). That nomenclature is driven by the idea that, at the so-called thermodynamic equilibrium, when dissipation is zero, the non-equilibrium energetic component vanishes. In other words, this component only contributes to the energy density under *out-of-equilibrium* conditions.

However, our goal is to operate within a broader mechanical framework in which the two components of the strain energy may be both different from zero at a steady state, when dissipation is zero. This scenario arises when forcing terms act on the internal-like viscous variables, allowing the system to reach a steady state, yet with both energetic components being nonzero. In such cases, the φ_{ov} component is responsible for overstresses which are necessary to maintain the equilibrium with the external forcing term. Therefore we prefer to label those energy components as φ and φ_{ov} as opposed to φ_{Eq} and φ_{NEq}.

3.2. Actual power and dissipation

In adherence to the principles of continuum thermodynamics, we introduce a specific dissipation density δ, which represents the disparity between the stress power per unit reference volume and the time rate of the elastic energy density, and require it to be non-negative for any admissible deformation rates $\dot{\mathbf{F}}$ and $\dot{\mathbf{F}}_v$. So, the dissipation inequality in local form reads:

$$\varrho_0 \, \delta = \mathbf{S} \cdot \dot{\mathbf{F}} + J_v \, \mathbf{G} \cdot \dot{\mathbf{F}}_v \mathbf{F}_v^{-1} - \varrho_0 \, \dot{\phi} \; \geq 0 \,. \tag{3.12}$$

The power is dissipated by the reference stress $\mathbf{S}$, also known as First Piola–Kirchhoff stress tensor, on the rate of deformation gradient. Simultaneously, the inner remodelling action $\mathbf{G}$ expends power on the viscous deformation rate tensor $\mathbf{L}_v$. It is imperative that the constitutive functions $\hat{\mathbf{S}}$ and $\hat{\mathbf{G}}$, delivering the reference stress $\mathbf{S}$ and the inner remodelling action $\mathbf{G}$, comply with the dissipation inequality (3.12). This adherence to the dissipation inequality is enforced through the Coleman-Noll procedure (Coleman and Noll, 1963), enabling the identification of a class of constitutive equations $\hat{\mathbf{S}}$ and $\hat{\mathbf{G}}$ that are thermodynamically consistent. By analysing the structure of the energy defined in Eq. (3.11), the time derivative of the specific energy, denoted as $\dot{\phi}$, can be expressed as follows:

$$\dot{\phi} = \frac{\partial \varphi}{\partial \mathbf{C}} \cdot \dot{\mathbf{C}} + \frac{\partial \varphi_{ov}}{\partial \mathbf{C}_e} \cdot \dot{\mathbf{C}}_e + \frac{\partial \varphi_{ov}}{\partial \mathbf{A}_v} \cdot \dot{\mathbf{A}}_v \,, \tag{3.13}$$

since the reference generalized orientation tensor $\mathbf{A}_0$ remains constant over time, i.e., $\dot{\mathbf{A}}_0 = \mathbf{0}$, but the same does not hold true for $\mathbf{A}_v$, which evolves in time as prescribed by Eq. (2.8).

Upon substitution of (2.6)–(2.8) and (3.13) into (3.12), and by using mass conservation, i.e., $\varrho_0 = J \, \varrho = J_v \, \varrho_v$, we get:

$$\varrho_0 \, \delta = \left(\mathbf{S} \mathbf{F}^T - 2 \varrho_0 \, \mathbf{F} \frac{\partial \varphi}{\partial \mathbf{C}} \mathbf{F}^T - 2 \varrho_0 \, \mathbf{F}_e \frac{\partial \varphi_{ov}}{\partial \mathbf{C}_e} \mathbf{F}_e^T \right) \cdot \mathbf{D}$$

$$+ J_v \left(\text{sym} \, \mathbf{G} + 2 \varrho_v \, \text{sym} \left(\mathbf{C}_e \frac{\partial \varphi_{ov}}{\partial \mathbf{C}_e} - \frac{\partial \varphi_{ov}}{\partial \mathbf{A}_v} \mathbf{A}_v \right) + 2 \varrho_v \left(\frac{\partial \varphi_{ov}}{\partial \mathbf{A}_v} \cdot \mathbf{A}_v \right) \mathbf{A}_v \right) \cdot \mathbf{D}_v$$

$$+ J_v \left(\text{skw} \, \mathbf{G} + \varrho_v \left([\mathbf{C}_e, \frac{\partial \varphi_{ov}}{\partial \mathbf{C}_e}] + [\mathbf{A}_v, \frac{\partial \varphi_{ov}}{\partial \mathbf{A}_v}] \right) \right) \cdot \mathbf{W}_v \geq 0 \,, \tag{3.14}$$

where, with a slight abuse of notation, we confused the function $\hat{\varphi}$ with the value φ it takes, and similarly for the other constitutive functions. Moreover, the square brackets indicate the commutator operator $[\mathbf{A}, \mathbf{B}] = \mathbf{A}\mathbf{B} - \mathbf{B}\mathbf{A}$ for any tensors $\mathbf{A}$ and $\mathbf{B}$. A consequence of this definition is that the commutator of two symmetric tensors is zero if and only if the two tensors are coaxial, implying that they share the same eigenvectors (Vianello, 1996; Ciambella and Nardinocchi, 2019).

We further assume that dissipation is solely associated with the viscous material behaviour and adhere to the inequality (3.14) by proposing the following simple constitutive equation for the First Piola–Kirchhoff stress $\mathbf{S}$:

$$\mathbf{S} = \mathbf{S}_e + \mathbf{S}_{ov}, \qquad \mathbf{S}_e = 2 \varrho_0 \, \mathbf{F} \frac{\partial \varphi}{\partial \mathbf{C}}, \qquad \mathbf{S}_{ov} = 2 \varrho_0 \, \mathbf{F}_e \frac{\partial \varphi_{ov}}{\partial \mathbf{C}_e} \mathbf{F}_v^{-T} \,. \tag{3.15}$$

Eq. (3.15) shows that the additive split of the elastic energy results in an additive split of the stress tensor. Indeed, the component $\mathbf{S}_e$ corresponds to the energetic contribution φ. Importantly, given that φ is non-zero for elastic strains being null, specifically when $\mathbf{F}_e = \mathbf{I}$, $\mathbf{S}_e$ controls the asymptotic material behaviour, particularly at the remodelled state. Additionally, it represents the sole stress component at the end of a viscous relaxation experiment. Conversely, the component $\mathbf{S}_{ov}$ is the *overstress* term, subject to relaxation through viscous processes. This representation of $\mathbf{S}$ extends the forces acting on parallel elements of the standard solid rheological model in three-dimensional, nonlinear viscoelasticity (refer, for instance, to Reese and Govindjee (1998)). As demonstrated in Ciambella and Nardinocchi (2021) (see the Appendix therein with $\varphi_{ov} \equiv \phi$), the following identity holds:

$$\left[\mathbf{C}_e, \frac{\partial \varphi_{ov}}{\partial \mathbf{C}_e} \right] + \left[\mathbf{A}_v, \frac{\partial \varphi_{ov}}{\partial \mathbf{A}_v} \right] = \mathbf{0} \,. \tag{3.16}$$

With Eqs. (3.15)–(3.16) on hands, we obtain the reduced dissipation inequality:

$$\varrho_0 \, \delta = J_v \, \text{skw} \, \mathbf{G} \cdot \mathbf{W}_v \tag{3.17}$$

$$+ J_v \left(\text{sym} \, \mathbf{G} + 2 \varrho_v \, \text{sym} \left(\mathbf{C}_e \frac{\partial \varphi_{ov}}{\partial \mathbf{C}_e} - \frac{\partial \varphi_{ov}}{\partial \mathbf{A}_v} \mathbf{A}_v \right) + 2 \varrho_v \left(\frac{\partial \varphi_{ov}}{\partial \mathbf{A}_v} \cdot \mathbf{A}_v \right) \mathbf{A}_v \right) \cdot \mathbf{D}_v \geq 0 \,,$$

which depends both on the viscous stretch rate $\mathbf{D}_v$ and on the viscous spin $\mathbf{W}_v$.

In Ciambella and Nardinocchi (2021), it was shown that for the dissipation to be consistent with SFI, the dissipation density must depend solely on the viscous stretch rate and not on the viscous spin. Therefore, to adhere to SFI, we introduce the following constitutive assumptions:

$$\text{skw} \, \mathbf{G} = \mathbf{0} \,, \tag{3.18}$$

$$\text{sym} \, \mathbf{G} = \mathbf{G}_{dis} + \mathbf{E}_{sh} \,. \tag{3.19}$$

The former guarantees that the dissipation is independent of $\mathbf{W}_v$, as required by SFI, whereas the latter assumes that the inner remodelling action is made of a dissipative part $\mathbf{G}_{dis}$ and of an energetic component $\mathbf{E}_{sh}$ known as the *Eshelby stress*, defined by:

$$\mathbf{E}_{sh} = -2 \varrho_v \, \text{sym} \left(\mathbf{C}_e \frac{\partial \varphi_{ov}}{\partial \mathbf{C}_e} - \frac{\partial \varphi_{ov}}{\partial \mathbf{A}_v} \mathbf{A}_v \right) - 2 \varrho_v \left(\frac{\partial \varphi_{ov}}{\partial \mathbf{A}_v} \cdot \mathbf{A}_v \right) \mathbf{A}_v \,. \tag{3.20}$$

As a result, the dissipation inequality is further reduced to:

$$\varrho_0 \, \delta = J_v \, \mathbf{G}_{dis} \cdot \mathbf{D}_v \geq 0 \,. \tag{3.21}$$

If the dissipation density δ is a quadratic function of the viscous stretch rate $\mathbf{D}_v$ and the generalized orientation tensor $\mathbf{A}_v$, i.e., $\delta = \delta(\mathbf{D}_v, \mathbf{A}_v)$[5], an appropriate constitutive representation of $\mathbf{G}_{dis}$ can be consequently derived. The most general quadratic form of two symmetric tensors involves five constitutive coefficients and can be expressed as:

$$\varrho_0 \, \delta(\mathbf{D}_v, \mathbf{A}_v) = \eta_1 J_1^2 + \eta_2 J_2 + \eta_3 J_1 J_4 + \eta_4 J_4^2 + \eta_5 J_5 \geq 0 \,, \tag{3.22}$$

with

$$J_1 = \mathbf{D}_v \cdot \mathbf{I}, \qquad J_2 = \mathbf{D}_v \cdot \mathbf{D}_v, \qquad J_4 = \mathbf{D}_v \cdot \mathbf{A}_v, \qquad J_5 = \mathbf{D}_v^2 \cdot \mathbf{A}_v,$$

the invariants of $\mathbf{D}_v$ and $\mathbf{A}_v$, in terms of the constitutive coefficients η_i, $i = 1, \ldots, 5$, ($[\eta_i] = \text{J s m}^{-3}$) which determine the dissipated power per unit reference volume. In particular, η_2 measures the shear viscosity parallel to the fibres, η_4 is the extensional viscosity along the fibre directions, η_5 is related to the relative viscosity for shear parallel and orthogonal to the fibres, and η_1, η_3 quantify viscosity associated with viscous volume variations (Spencer, 2004).

By direct comparison of (3.22) with (3.21), one obtains a possible constitutive equation for the dissipative symmetric part of the internal

---

5 To maintain consistency with SFI.

action[6]:

$$J_{\mathrm{v}}\,\mathbf{G}_{\mathrm{dis}} = \eta_1(\mathbf{D}_{\mathrm{v}} \cdot \mathbf{I})\mathbf{I} + \eta_2\mathbf{D}_{\mathrm{v}} + \eta_3\big((\mathbf{D}_{\mathrm{v}} \cdot \mathbf{A}_{\mathrm{v}})\mathbf{I} + (\mathbf{D}_{\mathrm{v}} \cdot \mathbf{I})\mathbf{A}_{\mathrm{v}}\big) \\ + \eta_4(\mathbf{D}_{\mathrm{v}} \cdot \mathbf{A}_{\mathrm{v}})\mathbf{A}_{\mathrm{v}} + \eta_5(\mathbf{D}_{\mathrm{v}}\mathbf{A}_{\mathrm{v}} + \mathbf{A}_{\mathrm{v}}\mathbf{D}_{\mathrm{v}})\,. \tag{3.23}$$

3.3. Balance equations and flow rule

The constitutive equations for the stress and the inner remodelling action must be used in the balance equations to get the evolution equations of the model. The standard balance equation of forces is written in its reference form as:

$$\mathrm{div}\,\mathbf{S} = \mathbf{0} \quad \text{in} \quad \Omega \qquad \text{and} \qquad \mathbf{S}\mathbf{n} = \mathbf{t}_0 \quad \text{on} \quad \partial\Omega\,, \tag{3.24}$$

where $\mathbf{t}_0$ is the boundary traction (per unit of reference area), $\mathbf{n}$ is the outward unit normal to $\partial\Omega$, and the bulk forces are assumed to vanish. On the other hand, no external actions are assumed to act on the inner viscous degrees of freedom and the balance equation of the remodelling action takes the simple form[7]:

$$\mathbf{G} = \mathbf{0} \quad \text{in} \quad \Omega\,, \tag{3.25}$$

as derived in Ciambella and Nardinocchi (2021). As a consequence, the constitutive Eq. (3.19) together with the balance Eq. (3.25) and the conservation of mass $\varrho_0 = J_{\mathrm{v}}\varrho_{\mathrm{v}}$, delivers the flow rule of the viscous stretch rate $\mathbf{D}_{\mathrm{v}}$:

$$\eta_1(\mathbf{D}_{\mathrm{v}} \cdot \mathbf{I})\mathbf{I} + \eta_2\mathbf{D}_{\mathrm{v}} + \eta_3\big((\mathbf{D}_{\mathrm{v}} \cdot \mathbf{A}_{\mathrm{v}})\mathbf{I} + (\mathbf{D}_{\mathrm{v}} \cdot \mathbf{I})\mathbf{A}_{\mathrm{v}}\big) + \eta_4(\mathbf{D}_{\mathrm{v}} \cdot \mathbf{A}_{\mathrm{v}})\mathbf{A}_{\mathrm{v}} \\ + \eta_5(\mathbf{D}_{\mathrm{v}}\mathbf{A}_{\mathrm{v}} + \mathbf{A}_{\mathrm{v}}\mathbf{D}_{\mathrm{v}}) = 2\varrho_0\,\mathrm{sym}\left(\mathbf{C}_{\mathrm{e}}\frac{\partial\varphi_{\mathrm{ov}}}{\partial\mathbf{C}_{\mathrm{e}}} - \frac{\partial\varphi_{\mathrm{ov}}}{\partial\mathbf{A}_{\mathrm{v}}}\mathbf{A}_{\mathrm{v}}\right) \\ + 2\varrho_0\left(\frac{\partial\varphi_{\mathrm{ov}}}{\partial\mathbf{A}_{\mathrm{v}}} \cdot \mathbf{A}_{\mathrm{v}}\right)\mathbf{A}_{\mathrm{v}}\,. \tag{3.26}$$

In order to determine $\mathbf{A}_{\mathrm{v}}$ in previous equation, one has to further prescribe an evolution for the skew symmetric part of the viscous rate. Following Ciambella and Nardinocchi (2021), here we assume that

$$\mathbf{W}_{\mathrm{v}} = \mathbf{0}\,, \tag{3.27}$$

and interpret it as an internal constraint enforced by null reactive actions, a consequence of Eq. (3.18) and the balance Eq. (3.25). Eq. (3.27) implies $\mathbf{L}_{\mathrm{v}} = \mathbf{D}_{\mathrm{v}}$, leading to $\dot{\mathbf{F}}_{\mathrm{v}} = \mathbf{D}_{\mathrm{v}}\mathbf{F}_{\mathrm{v}}$, which governs the remodelling process. The remodelled orientation is then determined from Eq. (2.8) as:

$$\dot{\mathbf{A}}_{\mathrm{v}} = \mathbf{D}_{\mathrm{v}}\mathbf{A}_{\mathrm{v}} + \mathbf{A}_{\mathrm{v}}\mathbf{D}_{\mathrm{v}} - 2(\mathbf{A}_{\mathrm{v}} \cdot \mathbf{D}_{\mathrm{v}})\mathbf{A}_{\mathrm{v}}\,, \qquad \mathbf{A}_{\mathrm{v}}(0) = \mathbf{A}_0\,. \tag{3.28}$$

The complete set of equations that govern the equilibrium of this continuum is summarized in Table 1. However, as we show in Section 4, we work with equations in referential form, avoiding the necessity of making assumptions on $\mathbf{W}_{\mathrm{v}}$ and the explicit computation of $\mathbf{A}_{\mathrm{v}}$.

Remark 4. It is noteworthy that Eq. (3.26) highlights the role of the Eshelby stress, i.e., the right-hand side of the equation dependent on the overstress energy density, in driving the evolution of the internal variable. In Ciambella and Nardinocchi (2021), it was demonstrated that for small elastic deformations, where $\mathbf{C}_{\mathrm{e}} = \mathbf{I} + 2\,\varepsilon\,\mathbf{E}_{\mathrm{e}}$, the Eshelby stress approaches the Cauchy stress and $\mathbf{D}_{\mathrm{v}}$ tends to $\mathbf{D}$ (at order ε). This implies that the previous equation represents the constitutive equation of an anisotropic Ericksen fluid, where particles rotate at the same angular velocity as the fluid line elements to which they are parallel (Ericksen, 1960). In contrast, other approaches in the literature, such as (Sadik and Yavari, 2024), assume the flow rule to be dependent on the reference orientation of the fibres; this implies that in the limit of small strain rates, the equivalent fluid model is unaffected by the viscous flow of the reinforcing particles.

Table 1
Recap of all modelling equations.

Balance	$\mathrm{div}\,\mathbf{S} = \mathbf{0}$ in Ω, $\quad$ $\mathbf{S}\mathbf{n} = \mathbf{t}_0$ on $\partial\Omega$ $\mathbf{G} = \mathbf{0}$ in Ω
Constitutive	First Piola–Kirchhoff stress: $\mathbf{S} = \mathbf{S}_{\mathrm{e}} + \mathbf{S}_{\mathrm{ov}}, \quad \mathbf{S}_{\mathrm{e}} = 2\varrho_0\mathbf{F}\frac{\partial\varphi}{\partial\mathbf{C}}, \quad \mathbf{S}_{\mathrm{ov}} = 2\varrho_0\mathbf{F}_{\mathrm{e}}\frac{\partial\varphi_{\mathrm{ov}}}{\partial\mathbf{C}_{\mathrm{e}}}\mathbf{F}_{\mathrm{v}}^{-\mathrm{T}}$ Eshelby stress: $\mathbf{E}_{\mathrm{sh}} = -2\varrho_{\mathrm{v}}\,\mathrm{sym}\left(\mathbf{C}_{\mathrm{e}}\frac{\partial\varphi_{\mathrm{ov}}}{\partial\mathbf{C}_{\mathrm{e}}} - \frac{\partial\varphi_{\mathrm{ov}}}{\partial\mathbf{A}_{\mathrm{v}}}\mathbf{A}_{\mathrm{v}}\right) - 2\varrho_{\mathrm{v}}\left(\frac{\partial\varphi_{\mathrm{ov}}}{\partial\mathbf{A}_{\mathrm{v}}} \cdot \mathbf{A}_{\mathrm{v}}\right)\mathbf{A}_{\mathrm{v}}$ Dissipative inner action: $J_{\mathrm{v}}\,\mathbf{G}_{\mathrm{dis}} = \eta_1(\mathbf{D}_{\mathrm{v}} \cdot \mathbf{I})\mathbf{I} + \eta_2\mathbf{D}_{\mathrm{v}} + \eta_3\big((\mathbf{D}_{\mathrm{v}} \cdot \mathbf{A}_{\mathrm{v}})\mathbf{I} + (\mathbf{D}_{\mathrm{v}} \cdot \mathbf{I})\mathbf{A}_{\mathrm{v}}\big)$ $\qquad + \eta_4(\mathbf{D}_{\mathrm{v}} \cdot \mathbf{A}_{\mathrm{v}})\mathbf{A}_{\mathrm{v}} + \eta_5(\mathbf{D}_{\mathrm{v}}\mathbf{A}_{\mathrm{v}} + \mathbf{A}_{\mathrm{v}}\mathbf{D}_{\mathrm{v}})$
Evolution	Viscous stretch rate: $\eta_1(\mathbf{D}_{\mathrm{v}} \cdot \mathbf{I})\mathbf{I} + \eta_2\mathbf{D}_{\mathrm{v}} + \eta_3\big((\mathbf{D}_{\mathrm{v}} \cdot \mathbf{A}_{\mathrm{v}})\mathbf{I} + (\mathbf{D}_{\mathrm{v}} \cdot \mathbf{I})\mathbf{A}_{\mathrm{v}}\big)$ $\qquad + \eta_4(\mathbf{D}_{\mathrm{v}} \cdot \mathbf{A}_{\mathrm{v}})\mathbf{A}_{\mathrm{v}} + \eta_5(\mathbf{D}_{\mathrm{v}}\mathbf{A}_{\mathrm{v}} + \mathbf{A}_{\mathrm{v}}\mathbf{D}_{\mathrm{v}}) = -J_{\mathrm{v}}\,\mathbf{E}_{\mathrm{sh}}$ Viscous spin: $\quad \mathbf{W}_{\mathrm{v}} = \mathbf{0}$

Remark 5. It is important to recognize that the indeterminacy of the viscous spin, inherent in the multiplicative decomposition of the deformation gradient, makes the value assigned to the viscous spin by the internal constraint (3.27) not affecting the solution of the problem. Indeed, we can determine the symmetric component $\mathbf{C}_{\mathrm{v}}^{1/2}$ (as detailed in Section 4) of the viscous deformation $\mathbf{F}_{\mathrm{v}} = \mathbf{R}_{\mathrm{v}}\mathbf{C}_{\mathrm{v}}^{1/2}$, whereas the orthogonal component $\mathbf{R}_{\mathrm{v}}$ of $\mathbf{F}_{\mathrm{v}}$ remains indeterminate regardless of the value of $\mathbf{W}_{\mathrm{v}}$.

4. Reference flow rule

By utilizing suitable pull-back, the equations governing the evolution of inelastic variables can be recast in their reference form. This yields a flow rule expressed solely in terms of the deformation measures $\mathbf{C}$ and $\mathbf{C}_{\mathrm{v}}$, and on the reference orientation tensor $\mathbf{A}_0$. These measures inherently disregard superimposed rotations on the remodelled state, implying that their evolution is independent of specifying $\mathbf{W}_{\mathrm{v}}$. Notably, this approach does not enable the complete determination of $\mathbf{F}_{\mathrm{v}}$ due to the inherent indeterminacy of the remodelled state, even if the current state of the body can be completely characterized.

To reformulate the flow rule, we firstly recall that

$$\dot{\mathbf{C}}_{\mathrm{v}} = 2\mathbf{F}_{\mathrm{v}}^{\mathrm{T}}\mathbf{D}_{\mathrm{v}}\mathbf{F}_{\mathrm{v}}\,, \tag{4.29}$$

and so pre-multiplication by $2\mathbf{F}_{\mathrm{v}}^{\mathrm{T}}$ and post-multiplication by $\mathbf{F}_{\mathrm{v}}$ allow us to rewrite Eq. (3.26) as:

$$\eta_1\,(\dot{\mathbf{C}}_{\mathrm{v}} \cdot \mathbf{C}_{\mathrm{v}}^{-1})\mathbf{C}_{\mathrm{v}} + \eta_2\,\dot{\mathbf{C}}_{\mathrm{v}} + \eta_3\left(\frac{\dot{\mathbf{C}}_{\mathrm{v}} \cdot \mathbf{A}_0}{\mathbf{C}_{\mathrm{v}} \cdot \mathbf{A}_0}\mathbf{C}_{\mathrm{v}} + \frac{\dot{\mathbf{C}}_{\mathrm{v}} \cdot \mathbf{C}_{\mathrm{v}}^{-1}}{\mathbf{C}_{\mathrm{v}} \cdot \mathbf{A}_0}\mathbf{C}_{\mathrm{v}}\mathbf{A}_0\mathbf{C}_{\mathrm{v}}\right) \tag{4.30}$$

$$+ \eta_4\frac{\dot{\mathbf{C}}_{\mathrm{v}} \cdot \mathbf{A}_0}{(\mathbf{C}_{\mathrm{v}} \cdot \mathbf{A}_0)^2}\mathbf{C}_{\mathrm{v}}\mathbf{A}_0\mathbf{C}_{\mathrm{v}} + \eta_5\left(\frac{\dot{\mathbf{C}}_{\mathrm{v}}\mathbf{A}_0\mathbf{C}_{\mathrm{v}}}{\mathbf{C}_{\mathrm{v}} \cdot \mathbf{A}_0} + \frac{\mathbf{C}_{\mathrm{v}}\mathbf{A}_0\dot{\mathbf{C}}_{\mathrm{v}}}{\mathbf{C}_{\mathrm{v}} \cdot \mathbf{A}_0}\right) = -2J_{\mathrm{v}}\mathbf{F}_{\mathrm{v}}^{\mathrm{T}}\mathbf{E}_{\mathrm{sh}}\mathbf{F}_{\mathrm{v}}\,.$$

To ensure transverse isotropy in the remodelled state and consequently satisfy SFI, the elastic energy density φ_{ov} must be defined solely in terms of the invariants of the tensors $\mathbf{C}_{\mathrm{e}}$ and $\mathbf{A}_{\mathrm{v}}$. We write:

$$\varphi_{\mathrm{ov}}(\mathbf{C}_{\mathrm{e}}, \mathbf{A}_{\mathrm{v}}) = \tilde{\varphi}_{\mathrm{ov}}(I_1^{\mathrm{e}}, I_2^{\mathrm{e}}, I_3^{\mathrm{e}}, I_4^{\mathrm{e}}, I_5^{\mathrm{e}})\,,$$

where the elastic invariants $I_1^{\mathrm{e}}, \ldots, I_5^{\mathrm{e}}$ are defined as:

$$I_1^{\mathrm{e}} = \mathbf{I} \cdot \mathbf{C}_{\mathrm{e}}\,, \qquad I_2^{\mathrm{e}} = \mathbf{I} \cdot \mathbf{C}_{\mathrm{e}}^*\,, \qquad I_3^{\mathrm{e}} = \det\mathbf{C}_{\mathrm{e}}\,, \\ I_4^{\mathrm{e}} = \mathbf{A}_{\mathrm{v}} \cdot \mathbf{C}_{\mathrm{e}}\,, \qquad I_5^{\mathrm{e}} = \mathbf{A}_{\mathrm{v}} \cdot \mathbf{C}_{\mathrm{e}}^2\,, \tag{4.31}$$

where a superscript $*$ denotes the cofactor. Through the kinematic relationships (2.4), these invariants can be rewritten as:

$$I_1^{\mathrm{e}} = \mathbf{C}_{\mathrm{v}}^{-1} \cdot \mathbf{C}\,, \qquad I_2^{\mathrm{e}} = \frac{1}{\det\mathbf{C}_{\mathrm{v}}}\mathbf{C}_{\mathrm{v}} \cdot \mathbf{C}^*\,, \qquad I_3^{\mathrm{e}} = \frac{\det\mathbf{C}}{\det\mathbf{C}_{\mathrm{v}}}\,, \\ I_4^{\mathrm{e}} = \frac{\mathbf{C} \cdot \mathbf{A}_0}{\mathbf{C}_{\mathrm{v}} \cdot \mathbf{A}_0}\,, \qquad I_5^{\mathrm{e}} = \frac{\mathbf{C}\,\mathbf{C}_{\mathrm{v}}^{-1}\mathbf{C} \cdot \mathbf{A}_0}{\mathbf{C}_{\mathrm{v}} \cdot \mathbf{A}_0}\,. \tag{4.32}$$

---

[6] For completeness, it is worth mentioning that a factor of 2 is sometimes incorporated into this equation (Spencer, 2004).

[7] Boundary conditions are absent, since we consider a remodelling theory of grade 0.

Subsequently, by incorporating the constitutive equation of the Eshelby stress from Eq. (3.20) and the additional calculations in the Appendix, the evolution Eq. (4.30) can be expressed solely in terms of the reference quantities $\mathbf{C}_v$, $\mathbf{C}$, and $\mathbf{A}_0$, allowing for its solution upon specifying the initial condition for $\mathbf{C}_v$:

$$
\eta_1\,(\dot{\mathbf{C}}_v \cdot \mathbf{C}_v^{-1})\mathbf{C}_v + \eta_2\,\dot{\mathbf{C}}_v + \eta_3\left(\frac{\dot{\mathbf{C}}_v \cdot \mathbf{A}_0}{\mathbf{C}_v \cdot \mathbf{A}_0}\mathbf{C}_v + \frac{\dot{\mathbf{C}}_v \cdot \mathbf{C}_v^{-1}}{\mathbf{C}_v \cdot \mathbf{A}_0}\mathbf{C}_v\mathbf{A}_0\mathbf{C}_v\right) \qquad (4.33)
$$
$$
+ \eta_4\,\frac{\dot{\mathbf{C}}_v \cdot \mathbf{A}_0}{(\mathbf{C}_v \cdot \mathbf{A}_0)^2}\mathbf{C}_v\mathbf{A}_0\mathbf{C}_v + \eta_5\left(\frac{\dot{\mathbf{C}}_v\mathbf{A}_0\mathbf{C}_v}{\mathbf{C}_v \cdot \mathbf{A}_0} + \frac{\mathbf{C}_v\mathbf{A}_0\dot{\mathbf{C}}_v}{\mathbf{C}_v \cdot \mathbf{A}_0}\right)
$$
$$
= 4\,\varrho_0\left[\varphi_{\mathrm{ov},1}\,\mathbf{I} + \varphi_{\mathrm{ov},2}\,(\mathbf{C}_v^{-1} \cdot \mathbf{C})\mathbf{I} - \varphi_{\mathrm{ov},2}\,\mathbf{C}\mathbf{C}_v^{-1}\right]\mathbf{C}
$$
$$
+ 4\,\varrho_0\varphi_{\mathrm{ov},3}\,\frac{\det \mathbf{C}}{\det \mathbf{C}_v}\mathbf{C}_v + 4\,\varrho_0\varphi_{\mathrm{ov},4}\,\frac{\mathbf{C} \cdot \mathbf{A}_0}{(\mathbf{C}_v \cdot \mathbf{A}_0)^2}\mathbf{C}_v\mathbf{A}_0\mathbf{C}_v
$$
$$
+ 4\,\varrho_0\varphi_{\mathrm{ov},5}\left(\frac{\mathbf{C}\mathbf{A}_0\mathbf{C}}{\mathbf{C}_v \cdot \mathbf{A}_0} + \frac{\mathbf{C}\mathbf{C}_v^{-1}\mathbf{C} \cdot \mathbf{A}_0}{(\mathbf{C}_v \cdot \mathbf{A}_0)^2}\mathbf{C}_v\mathbf{A}_0\mathbf{C}_v\right).
$$

Here, $\varphi_{\mathrm{ov},i}$ indicates the derivative of the overstress energy density with respect to the ith invariant, whereas derivatives of the invariants are computed in Appendix.

To complete the reference form of the problem, one can compute the First Piola–Kirchhoff stress tensor expressed in terms of the referential quantities $\mathbf{C}_v$ and $\mathbf{A}_0$ and of the deformation measures $\mathbf{F}$ and $\mathbf{C}$. By utilizing the constitutive Eqs. (3.15) and the definitions (4.32) along with the derivatives provided in the Appendix, we arrive at the following expression:

$$
\mathbf{S}_e = 2\,\varrho_0\left(\varphi_{,1}\,\mathbf{F} + \varphi_{,2}\,(\mathbf{I} \cdot \mathbf{C})\mathbf{F} - \varphi_{,2}\,\mathbf{F}\mathbf{C} + \varphi_{,3}\,\mathbf{F}\mathbf{C}^*\right.
$$
$$
\left. + \varphi_{,4}\,\mathbf{F}\mathbf{A}_0 + \varphi_{,5}\,(\mathbf{F}\mathbf{A}_0\mathbf{C} + \mathbf{F}\mathbf{C}\mathbf{A}_0)\right) \qquad (4.34)
$$

and

$$
\mathbf{S}_{\mathrm{ov}} = 2\,\varrho_0\left(\varphi_{\mathrm{ov},1}\,\mathbf{I} + \varphi_{\mathrm{ov},2}\,(\mathbf{C}_v^{-1} \cdot \mathbf{C})\right)\mathbf{F}\mathbf{C}_v^{-1} - 2\,\varrho_0\,\varphi_{\mathrm{ov},2}\,\mathbf{F}\mathbf{C}_v^{-1}\mathbf{C}\mathbf{C}_v^{-1}
$$
$$
+ 2\,\varrho_0\,\varphi_{\mathrm{ov},3}\,\frac{\det \mathbf{C}}{\det \mathbf{C}_v}\mathbf{F}^{-\mathrm{T}} + 2\,\varrho_0\,\varphi_{\mathrm{ov},4}\,\frac{\mathbf{F}\mathbf{A}_0}{\mathbf{C}_v \cdot \mathbf{A}_0} \qquad (4.35)
$$
$$
+ 2\,\varrho_0\,\frac{\varphi_{\mathrm{ov},5}}{\mathbf{C}_v \cdot \mathbf{A}_0}\left(\mathbf{F}\mathbf{A}_0\mathbf{C}\mathbf{C}_v^{-\mathrm{T}} + \mathbf{F}\mathbf{C}_v^{-1}\mathbf{C}\mathbf{A}_0\right),
$$

that can be evaluated once the displacement $\mathbf{u}$ has been determined from the balance Eq. (3.24), allowing us to calculate $\mathbf{F}$, $\mathbf{C}$, and consequently $\mathbf{C}_v$ from (4.33).

4.1. Variational form of the flow rule

To address the numerical treatment of the problem, we employ a staggered numerical scheme. Before delving into the numerical implementation, we first show that the referential flow rule (4.33) can be formulated in a variational form. This approach, prevalent in various fields such as hydrodynamics, polymer science, and soft matter physics, involves representing the evolution equation for a state variable $\mathbf{H}$ using dissipative Ψ and elastic Φ potentials:

$$
\frac{\partial \Psi}{\partial \dot{\mathbf{H}}} + \frac{\partial \Phi}{\partial \mathbf{H}} = \mathbf{0}, \qquad (4.36)
$$

where it is assumed that $\Psi = \Psi(\mathbf{F}, \mathbf{H}, \dot{\mathbf{H}})$ and $\Phi = \Phi(\mathbf{F}, \mathbf{H})$. The evolution Eq. (4.36) for the variable $\mathbf{H}$ is the Euler–Lagrange equation corresponding to the minimization of the *Rayleighian* functional

$$
\mathcal{R}(\mathbf{F}, \dot{\mathbf{F}}, \mathbf{H}, \dot{\mathbf{H}}) := \Psi(\mathbf{F}, \mathbf{H}, \dot{\mathbf{H}}) + \dot{\Phi}(\mathbf{F}, \dot{\mathbf{F}}, \mathbf{H}, \dot{\mathbf{H}}) \qquad (4.37)
$$

with respect to the rate $\dot{\mathbf{H}}$, a procedure also known as *Onsager variational principle* (Doi, 2021, 2011). In particular, in analogy with Onsager's theory for irreversible isothermal thermodynamical processes, the evolution of the state variable $\dot{\mathbf{H}}$ is provided by the solution of a minimum problem, coupled with the elastic one.[8] A flow rule in the

---

[8] In this respect, we note that the derivative of $\mathcal{R}$ with respect to $\dot{\mathbf{F}}$ provides the constitutive equation for the first Piola stress $\mathbf{S}$.

form of Eq. (4.36) is also found in works that deal with viscoelasticity by using the so-called two-potential framework, see for instance (Kumar and Lopez-Pamies, 2016; Sadik and Yavari, 2024).

Here, we present a similar variational structure for the reference evolution Eq. (4.33) which, to our knowledge, has not been derived previously for viscoelastic materials. Such a formulation is relevant from a computational viewpoint, since it can be easily implemented in a finite element code, as we will discuss later. At the same time, it is theoretically interesting, as it integrates into the Onsager variational framework and pursues the goal of modelling viscoelasticity by means of a kinematic descriptor that does not require the explicit computation of $\mathbf{F}_v$. Specifically, we now show that Eq. (4.33) is equivalent to the following:

$$
\frac{\partial \Psi}{\partial \dot{\mathbf{C}}_v^{-1}} + \frac{\partial \Phi}{\partial \mathbf{C}_v^{-1}} = \mathbf{0}, \qquad (4.38)
$$

where

$$
\dot{\mathbf{C}}_v^{-1} := \frac{\mathrm{d}}{\mathrm{d}t}\left(\mathbf{C}_v^{-1}\right) = -\mathbf{C}_v^{-1}\dot{\mathbf{C}}_v\mathbf{C}_v^{-1}, \qquad (4.39)
$$

and the Onsager principle is formulated to determine the evolution of $\mathbf{C}_v^{-1}$. In detail, by using Eq. (4.39), the left-hand side of Eq. (4.33) can be rewritten as

$$
-\eta_1\,(\dot{\mathbf{C}}_v^{-1} \cdot \mathbf{C}_v)\mathbf{C}_v - \eta_2\,\mathbf{C}_v\dot{\mathbf{C}}_v^{-1}\mathbf{C}_v
$$
$$
-\eta_3\left(\frac{\dot{\mathbf{C}}_v^{-1} \cdot \mathbf{C}_v\mathbf{A}_0\mathbf{C}_v}{\mathbf{C}_v \cdot \mathbf{A}_0}\mathbf{C}_v + \frac{\mathbf{C}_v \cdot \dot{\mathbf{C}}_v^{-1}}{\mathbf{C}_v \cdot \mathbf{A}_0}\mathbf{C}_v\mathbf{A}_0\mathbf{C}_v\right)
$$
$$
-\eta_4\,\frac{\mathbf{C}_v\mathbf{A}_0\mathbf{C}_v \cdot \dot{\mathbf{C}}_v^{-1}}{(\mathbf{C}_v \cdot \mathbf{A}_0)^2}\mathbf{C}_v\mathbf{A}_0\mathbf{C}_v - \eta_5\left(\frac{\mathbf{C}_v\dot{\mathbf{C}}_v^{-1}\mathbf{C}_v\mathbf{A}_0\mathbf{C}_v}{\mathbf{C}_v \cdot \mathbf{A}_0} + \frac{\mathbf{C}_v\mathbf{A}_0\mathbf{C}_v\dot{\mathbf{C}}_v^{-1}\mathbf{C}_v}{\mathbf{C}_v \cdot \mathbf{A}_0}\right)
$$
$$
= \frac{\partial \Psi}{\partial \dot{\mathbf{C}}_v^{-1}}. \qquad (4.40)
$$

The dissipative potential $\Psi(\dot{\mathbf{C}}_v^{-1}, \mathbf{C}_v, \mathbf{A}_0)$ is defined by

$$
\Psi(\dot{\mathbf{C}}_v^{-1}, \mathbf{C}_v, \mathbf{A}_0) = \frac{1}{2}\dot{\mathbf{C}}_v^{-1} \cdot \mathbb{D}(\mathbf{C}_v, \mathbf{A}_0)\dot{\mathbf{C}}_v^{-1}, \qquad (4.41)
$$

with the fourth-order positive-definite tensor $\mathbb{D}(\mathbf{C}_v, \mathbf{A}_0)$ given by

$$
\mathbb{D}(\mathbf{C}_v, \mathbf{A}_0) = \eta_1\,\mathbf{C}_v \otimes \mathbf{C}_v + \eta_2\,\mathbf{C}_v\,\overline{\underline{\otimes}}\,\mathbf{C}_v
$$
$$
+ \eta_3\left(\mathbf{C}_v \otimes \frac{\mathbf{C}_v\mathbf{A}_0\mathbf{C}_v}{\mathbf{C}_v \cdot \mathbf{A}_0} + \frac{\mathbf{C}_v\mathbf{A}_0\mathbf{C}_v}{\mathbf{C}_v \cdot \mathbf{A}_0} \otimes \mathbf{C}_v\right)
$$
$$
+ \eta_4\,\frac{\mathbf{C}_v\mathbf{A}_0\mathbf{C}_v}{(\mathbf{C}_v \cdot \mathbf{A}_0)^2} \otimes \mathbf{C}_v\mathbf{A}_0\mathbf{C}_v + \eta_5\left(\mathbf{C}_v\,\overline{\underline{\otimes}}\,\frac{\mathbf{C}_v\mathbf{A}_0\mathbf{C}_v}{\mathbf{C}_v \cdot \mathbf{A}_0} + \frac{\mathbf{C}_v\mathbf{A}_0\mathbf{C}_v}{\mathbf{C}_v \cdot \mathbf{A}_0}\,\overline{\underline{\otimes}}\,\mathbf{C}_v\right),
$$
$$
\qquad (4.42)
$$

and η_i are the viscosities introduced in Eq. (3.22). The following notation was used:

$$
(\mathbf{A}\,\overline{\otimes}\,\mathbf{B})\mathbf{C} = \mathbf{A}\mathbf{C}\mathbf{B}^{\mathrm{T}}, \quad (\mathbf{A}\,\underline{\otimes}\,\mathbf{B})\mathbf{C} = \mathbf{A}\mathbf{C}^{\mathrm{T}}\mathbf{B}^{\mathrm{T}}, \quad \mathbf{A}\,\overline{\underline{\otimes}}\,\mathbf{B} = \frac{1}{2}(\mathbf{A}\,\overline{\otimes}\,\mathbf{B} + \mathbf{A}\,\underline{\otimes}\,\mathbf{B}).
$$

If we additionally define

$$
\Phi(\mathbf{C}, \mathbf{C}_v^{-1}, \mathbf{A}_0) = 4\varrho_0\,\varphi_{\mathrm{ov}}(\mathbf{C}, \mathbf{C}_v^{-1}, \mathbf{A}_0) + 4\varrho_0\,\varphi(\mathbf{C}, \mathbf{A}_0), \qquad (4.43)
$$

i.e., we consider the overstress free energy as a function of the state variable $\mathbf{C}_v^{-1}$, it is immediate to observe that the right-hand side of Eq. (4.33) can be restated as

$$
4\varrho_0\left[\varphi_{\mathrm{ov},1}\,\mathbf{I} + \varphi_{\mathrm{ov},2}\,(\mathbf{C}_v^{-1} \cdot \mathbf{C})\mathbf{I} - \varphi_{\mathrm{ov},2}\,\mathbf{C}\mathbf{C}_v^{-1}\right]\mathbf{C}
$$
$$
+ 4\,\varrho_0\varphi_{\mathrm{ov},3}\,\frac{\det \mathbf{C}}{\det \mathbf{C}_v}\mathbf{C}_v + 4\,\varrho_0\,\varphi_{\mathrm{ov},4}\,\frac{\mathbf{C} \cdot \mathbf{A}_0}{(\mathbf{C}_v \cdot \mathbf{A}_0)^2}\mathbf{C}_v\mathbf{A}_0\mathbf{C}_v
$$
$$
+ 4\,\varrho_0\varphi_{\mathrm{ov},5}\left(\frac{\mathbf{C}\mathbf{A}_0\mathbf{C}}{\mathbf{C}_v \cdot \mathbf{A}_0} + \frac{\mathbf{C}\mathbf{C}_v^{-1}\mathbf{C} \cdot \mathbf{A}_0}{(\mathbf{C}_v \cdot \mathbf{A}_0)^2}\mathbf{C}_v\mathbf{A}_0\mathbf{C}_v\right) = -\frac{\partial \Phi}{\partial \mathbf{C}_v^{-1}}. \qquad (4.44)
$$

Therefore, our referential flow rule (4.33) can be recast in the variational form of Eq. (4.38), with the dissipative and elastic potentials given by Eqs. (4.41) and (4.43), respectively. The state variable of the variational problem is therefore the *inverse viscous strain* $\mathbf{C}_v^{-1}$ and the

evolution law is equivalent to finding, for a given deformation $\mathbf{C}$ and an initial fibre distribution $\mathbf{A}_0$, the value of $\mathbf{C}_v^{-1}$ that satisfies the minimum problem in the appropriate space[9]:

$$\min_{\dot{\mathbf{C}}_v^{-1}} \left\{ \frac{\partial \Phi}{\partial \mathbf{C}_v^{-1}} \cdot \dot{\mathbf{C}}_v^{-1} + \Psi\left(\dot{\mathbf{C}}_v^{-1}, \mathbf{C}_v^{-1}, \mathbf{A}_0\right) \right\}. \tag{4.45}$$

Previous variational structure facilitates a direct numerical implementation of the model. In particular, by following the procedure also used in Miehe et al. (2004), Fancello et al. (2006) and Ortiz and Stainier (1999), we assume that the time interval $[0, T]$ is subdivided into a sequence of time steps $0 = t_0 < t_1 < \cdots < t_n < t_{n+1} < \cdots < t_N = T$ such that $\Delta t = t_{n+1} - t_n$ is the time increment. We can then evaluate the incremental work done on the system during the interval $[t_n, t_{n+1}]$ as:

$$\mathcal{W}_{n+1} = \int_{t_n}^{t_{n+1}} \left(\dot{\Phi} + \Psi\right) dt = \Phi^{n+1} - \Phi^n + \Delta t \, \Psi\left(\overset{\circ}{\mathbf{C}}_v^{-1}, [\mathbf{C}_v]^n, \mathbf{A}_0\right), \tag{4.46}$$

where $\Phi^{n+1} = \Phi([\mathbf{C}]^{n+1}, [\mathbf{C}_v]^{n+1}, \mathbf{A}_0)$, $\Phi^n = \Phi([\mathbf{C}]^n, [\mathbf{C}_v]^n, \mathbf{A}_0)$, and $\overset{\circ}{\mathbf{C}}_v^{-1}$ is a suitable incremental approximation of $\dot{\mathbf{C}}_v^{-1}$. The continuous variational problem (4.45) on the interval $[t_n, t_{n+1}]$ is then equivalent to minimizing such an incremental work, that is,

$$\min_{[\mathbf{C}_v^{-1}]^{n+1}} \left\{ \Phi\left([\mathbf{C}]^{n+1}, [\mathbf{C}_v^{-1}]^{n+1}, \mathbf{A}_0\right) + \Delta t \, \Psi\left([\mathbf{C}_v^{-1}]^{n+1}, [\mathbf{C}_v^{-1}]^n, \mathbf{A}_0\right) \right\}. \tag{4.47}$$

Hence, given the deformation $[\mathbf{C}]^{n+1}$ at the next time step t_{n+1}, Eq. (4.47) provides the value of the unknown state variable $[\mathbf{C}_v^{-1}]^{n+1}$.

The numerical implementation of the problem is achieved through a staggered algorithm with an iterative alternate minimization procedure, summarized in Algorithm 1. Starting from the solution $([\mathbf{C}]^n, [\mathbf{C}_v^{-1}]^n)$ at previous step, we firstly solve the nonlinear elastic problem with given $[\mathbf{C}_v^{-1}]^n$ to find $[\mathbf{C}]^{n+1}$ through the minimization

$$[\mathbf{C}]^{n+1} = \arg\min_{\mathbf{C}} \Phi\left(\mathbf{C}, [\mathbf{C}_v^{-1}]^n, \mathbf{A}_0\right), \tag{4.48}$$

in the absence of external forces. If external forces are present, we augment the objective function with the external work. Then, we use this value of $[\mathbf{C}]^{n+1}$ to solve the variational problem (4.47) for $[\mathbf{C}_v^{-1}]^{n+1}$. The procedure is iterated until variations in $[\mathbf{C}_v^{-1}]^{n+1}$ are below a fixed tolerance or a maximum number of iterations is reached.

Remark 6. To compute the first Piola stress tensor $[\mathbf{S}]^{n+1}$ at time t_{n+1}, recalling Eqs. (4.34)–(4.35), it is actually required to know $[\mathbf{F}]^{n+1}$ in addition to $[\mathbf{C}]^{n+1}$. Therefore, in the numerical computations, we solve the elastic problem (4.48) with respect to the displacement field $\mathbf{u}(X, t)$ and then we use it to evaluate the deformation gradient.

5. Numerical examples and benchmark problems

We show the application of the model in simplified settings, through the analysis of some benchmark problems in viscoelasticity. Specifically, we consider a viscoelastic anisotropic body reinforced with a distribution of fibres and simulate stress relaxation and recovery, cyclic deformation tests, and creep tests. These three cases allow to highlight the main features of the viscoelastic model in different experimental conditions. Finally, we simulate a simple shear condition, to take into account also a case in which the problem is not homogeneous.

In detail, introduced an orthonormal basis $(\mathbf{e}_1, \mathbf{e}_2, \mathbf{e}_3)$, we consider a material with a distribution of fibres in the reference configuration characterized by the generalized orientation tensor

$$\mathbf{A}_0 = \mathrm{diag}(0.1, 0.2, 0.7), \tag{5.49}$$

so that the majority of fibres is found along the direction $\mathbf{e}_3$. For simplicity, we choose both the components of the strain energy in

---

Algorithm 1 Staggered algorithm for the coupled viscoelastic problem in referential form

1: $n = 0$
2: **while** $t \leq T$ **do**
3:   $t \mathrel{+}= \Delta t$
4:   Given $([\mathbf{C}]^n, [\mathbf{C}_v^{-1}]^n)$, solve (4.48) to find $[\mathbf{C}]_{\mathrm{iter}}^{n+1}$
5:   Given $([\mathbf{C}]_{\mathrm{iter}}^{n+1}, [\mathbf{C}_v^{-1}]^n)$, solve (4.38) to find $[\mathbf{C}_v^{-1}]_{\mathrm{iter}}^{n+1}$
6:   $[\mathbf{C}_v^{-1}]_{\mathrm{trial}} \leftarrow [\mathbf{C}_v^{-1}]^n$
7:   **while** $\|[\mathbf{C}_v^{-1}]_{\mathrm{trial}} - [\mathbf{C}_v^{-1}]_{\mathrm{iter}}^{n+1}\| > \mathrm{tol}$ **and** numiter $<$ itermax **do**
8:    $[\mathbf{C}_v^{-1}]_{\mathrm{trial}} \leftarrow [\mathbf{C}_v^{-1}]_{\mathrm{iter}}^{n+1}$ and $[\mathbf{C}]_{\mathrm{trial}} \leftarrow [\mathbf{C}]_{\mathrm{iter}}^{n+1}$
9:    Given $([\mathbf{C}]_{\mathrm{trial}}, [\mathbf{C}_v^{-1}]_{\mathrm{trial}})$, solve (4.48) to find $[\mathbf{C}]_{\mathrm{iter}}^{n+1}$
10:    Given $([\mathbf{C}]_{\mathrm{iter}}^{n+1}, [\mathbf{C}_v^{-1}]_{\mathrm{trial}})$, solve (4.38) to find $[\mathbf{C}_v^{-1}]_{\mathrm{iter}}^{n+1}$
11:   **end while**
12:   $[\mathbf{C}]^n \leftarrow [\mathbf{C}]_{\mathrm{iter}}^{n+1}$ and $[\mathbf{C}_v^{-1}]^n \leftarrow [\mathbf{C}_v^{-1}]_{\mathrm{iter}}^{n+1}$
13:   $n \mathrel{+}= 1$
14: **end while**

Table 2
Constitutive parameters used in the simulations.

$\mu = 13.54$ kPa	$\kappa = 13.5$ MPa	$\gamma = 0.2$
$\mu_{\mathrm{ov}} = 5.4$ kPa	$\kappa_{\mathrm{ov}} = 13.5$ MPa	$\gamma_{\mathrm{ov}} = 0.2$

the form of Neo-Hookean elastic energies with a standard reinforcing component, namely,

$$\varrho_0 \, \varphi(I_1, I_3, I_4) = \frac{\mu}{2}(I_1 - 3) - \mu \ln J + \frac{\kappa}{2}(J - 1)^2 + \frac{1}{2}\mu\gamma(I_4 - 1)^2, \tag{5.50}$$

$$\varrho_0 \, \varphi_{\mathrm{ov}}(I_1^{\mathrm{e}}, I_3^{\mathrm{e}}, I_4^{\mathrm{e}}) = \frac{\mu_{\mathrm{ov}}}{2}(I_1^{\mathrm{e}} - 3) - \mu_{\mathrm{ov}} \ln J_{\mathrm{e}} + \frac{\kappa_{\mathrm{ov}}}{2}(J_{\mathrm{e}} - 1)^2 + \frac{1}{2}\mu_{\mathrm{ov}}\gamma_{\mathrm{ov}}(I_4^{\mathrm{e}} - 1)^2. \tag{5.51}$$

In previous equations, μ, μ_{ov} denote the shear moduli of the material in its reference configuration, and $\kappa, \kappa_{\mathrm{ov}}$ are the reference bulk moduli with the dependence on J and J_{e} included in the energies to ensure that the material resists a pure volumetric compression. Specifically, the dependence on J_{e} alongside the one on J avoids excessive volume variations related to viscous effects. Moreover, $\gamma, \gamma_{\mathrm{ov}} \geq 0$ control the resistance of the elastic fibre distribution to stretch. We remark that, as discussed in Section 3.1, anisotropy is weighed in the overstress energy φ_{ov} by means of the remodelled structural tensor $\mathbf{A}_{\mathrm{v}}$, whence the dependence on I_4^{e}. The values of the material parameters that appear in the energies employed in the simulations are reported in Table 2. Furthermore, we introduce the characteristic times $\tau_1, \ldots, \tau_5$ associated with the viscosities that appear in Eq. (4.33) by setting $\eta_i = \mu_{\mathrm{ov}}\tau_i$, $i = 1, \ldots, 5$. With these choices, we solve the elastic problem and the flow rule by using the algorithmic procedure detailed in Section 4.1. In particular, implementation is performed by means of the Python-based Finite Element library *FEniCS* (Logg et al., 2012; Alnæs et al., 2015).

5.1. Uniaxial tests

We start simulating uniaxial experimental tests on a viscoelastic cube, with $\tau_2 = 1000$ s and $\tau_1 = \tau_3 = \tau_4 = \tau_5 = 0$. The first benchmark case that we consider is a stress relaxation experiment with recovery. The specimen is subjected to a sudden stretch $\lambda_{\mathrm{max}} = 3$ in the direction $\mathbf{e}_3$, which is the one with the highest fraction of fibres, whereas in the other two directions traction-free conditions are applied. The stretch is kept fixed for $t = 2000$ s, after which it is removed and recovery is observed for additional 1000 s.

The deformation history is shown in Fig. 2a, while the results for the S_{33} component of the first Piola–Kirchhoff stress are reported in Fig. 2b. It can be observed that, after an initial stress peak due to
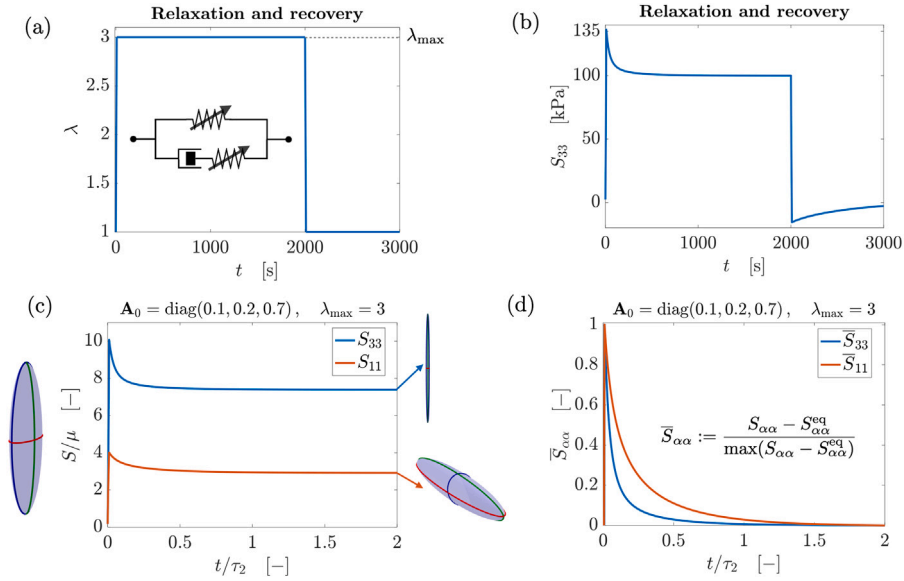
---

[9] We note that, with the definition of Eq. (4.43) the derivative of Φ with respect to $\mathbf{C}$ is equal to two times the second Piola–Kirchhoff stress tensor.

Fig. 2. Stress relaxation and recovery simulation. (a): applied deformation in time along the direction $\mathbf{e}_3$. (b): evolution of the stress component S_{33}. (c): magnification of the stress relaxation phase, with stress normalized with respect to μ and time with respect to τ_2. The ellipsoid on the left-hand side shows the fibre distribution $\mathbf{A}_0$, whereas the ellipsoids on the right-hand side show the final remodelled distributions. (d): plot of the normalized stress measure $\bar{S}_{\alpha\alpha}$. (For interpretation of the references to colour in this figure legend, the reader is referred to the web version of this article.)

the elastic instantaneous response, stress relaxation occurs. Yet, the material does not relax to a zero-stress state, owing to the presence of the energetic term φ, that represents the elastic spring in parallel with the Maxwell element in the rheological scheme in Fig. 1b. After the stretch is removed, the stress rapidly decreases and becomes negative, then it progressively returns to the initial stress-free state. Fig. 2c shows a magnification of the stress relaxation phase of the experiment. Stress values are normalized with respect to the shear modulus μ, whereas time is rescaled with the characteristic time τ_2. Additionally, the blue curve represents the stress component in the direction $\mathbf{e}_3$, while the red curve refers to an experiment where the same stretch is applied in the direction $\mathbf{e}_1$. As expected, the stress peak in S_{33} is more than doubled compared with the one in S_{11}, since the majority of reinforcing fibres are found along $\mathbf{e}_3$ and the material is more rigid in that direction. The initial ellipsoid associated with the fibre distribution (5.49) and the final ellipsoids are also shown in the plots. At the end of the relaxation phase, if the stretch is applied along $\mathbf{e}_3$, the distribution has become almost perfectly aligned with such a direction. Instead, coherently with the affine evolution of the fibres embedded in Eq. (2.3), a stretch applied along $\mathbf{e}_1$ makes the distribution elongate in this direction.

Finally, in Fig. 2d we highlight the nonlinearity of the relaxation time by plotting a rescaled measure of stress calculated as $\bar{S}_{\alpha\alpha} := (S_{\alpha\alpha} - S_{\alpha\alpha}^{\text{eq}})/\max(S_{\alpha\alpha} - S_{\alpha\alpha}^{\text{eq}})$, where $S_{\alpha\alpha}^{\text{eq}}$ is the value of the stress at steady state and $\alpha = 1, 3$. In this Figure, the distinct relaxation times correspond to uniaxial tractions along the directions of the highest and lowest fibre concentrations, denoted by $\mathbf{e}_3$ and $\mathbf{e}_1$, respectively. Specifically, the more rapid relaxation occurs in the direction where the specimen exhibits greater stiffness.

We also simulated a cyclic deformation experiment, where a triangular stretch

$$\lambda(t) = \begin{cases} 1 + |\dot{\lambda}|t & \text{if} \quad 0 < t \le T/2 \\ 3 - |\dot{\lambda}|(t - T/2) & \text{if} \quad T/2 < t \le T \end{cases} \tag{5.52}$$

is applied in the direction $\mathbf{e}_3$ as shown in Fig. 3(a). In particular, once the stretch rate $|\dot{\lambda}|$ is fixed, the duration T of the experiment is chosen in such a way that $\lambda(T/2) = 3$. In Fig. 3(b) we report the stretch-stress diagrams for different values of $|\dot{\lambda}|$. We firstly observe that two elastic limits exist, for high and low stretch rates. In the former case, with reference to Eq. (3.15) and to the blue curve in Fig. 3(b), we have
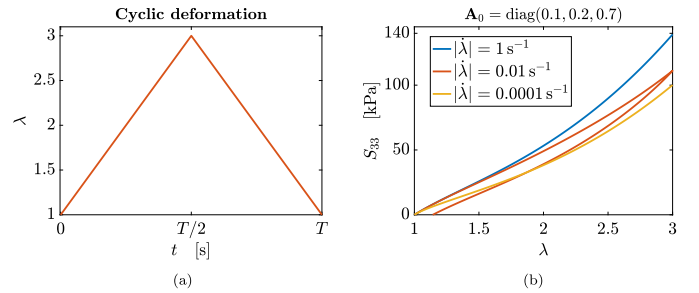

Fig. 3. Cyclic deformation test. (a): applied stretch λ as a function of time, as given by Eq. (5.52). (b): stretch-stress curves in the direction $\mathbf{e}_3$ for different values of the stretch rate $|\dot{\lambda}|$. (For interpretation of the references to colour in this figure legend, the reader is referred to the web version of this article.)

that no dissipation occurs, and the total stress follows the one of a hyperelastic body with strain energy given by the sum of the elastic and overstress energies, i.e.,

$$\mathbf{S} \approx 2\varrho_0 \mathbf{F} \frac{\partial}{\partial \mathbf{C}}(\varphi + \varphi_{\text{ov}}), \tag{5.53}$$

taking into account that $\mathbf{F}_{\text{e}} \to \mathbf{F}$. Instead, for very low stretch rate, corresponding to the yellow curve in Fig. 3(b), another elastic branch is found, owing to the presence of a spring component in parallel with the dissipative one. In this case, $\mathbf{F}_{\text{e}} \to \mathbf{I}$ and the first Piola stress is given by

$$\mathbf{S} \approx 2\varrho_0 \mathbf{F} \frac{\partial \varphi}{\partial \mathbf{C}}, \tag{5.54}$$

with the overstress component that vanishes. Between these two limits, the material exhibits a hysteretic behaviour, due to viscous relaxation processes.

The last situation that we simulate is a creep and recovery experiment, which is relevant for viscoelastic biological tissues like the reproductive tissue tested in Dubik et al. (2022) and Clark-Patterson et al. (2021). In this case, as shown in Fig. 4(a), we apply a constant traction S in the direction $\mathbf{e}_3$, which is held fixed for 2000 s. A second creep step is then applied, with the traction being doubled and kept constant for additional 2000 s. Finally, the body is unloaded, in order to
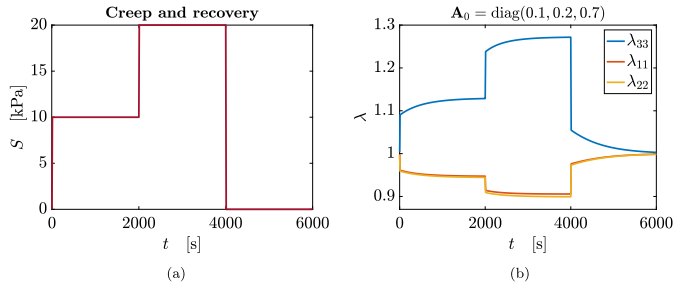
Fig. 4. Creep and recovery experiment for $\mathbf{A}_0 = \mathrm{diag}(0.1, 0.2, 0.7)$. (a): load history in the direction $\mathbf{e}_3$. A traction S of 10 kPa is suddenly applied to the specimen and maintained constant for 2000 s, then it is doubled and sustained for additional 2000 s. Afterwards, the load is removed and recovery is observed. (b): stretch response of the material to the applied traction shown in (a) in terms of the stretches λ_{11}, λ_{22}, and λ_{33} along the principal axes of the specimen.
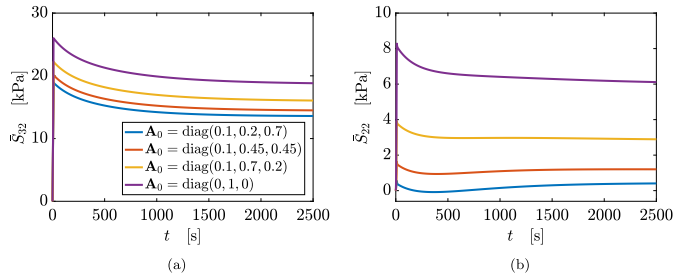

Fig. 5. Simple shear simulations for different initial distributions of fibres. (a): average stress $\bar{S}_{32}$. (b): average stress $\bar{S}_{22}$.

observe the recovery phase. Results in terms of the stretch components λ_{11}, λ_{22}, and λ_{33} are shown in Fig. 4(b). After the application of the force, the deformation in the loading direction continues to increase in both creep steps. Then, when the load is removed, the stretch λ_{33} undergoes an instantaneous elastic recovery, after which it progressively returns to the undeformed state. An opposite behaviour is observed for λ_{11} and λ_{22}, that decrease below 1 during creep, and then increase during the recovery phase.

5.2. Simple shear

To simulate a case in which stress and strain are not homogeneous, we perform simple shear finite element simulations of a rectangular specimen with square cross section, whose reference configuration is defined by

$$\Omega = \{(X_1, X_2, X_3) \mid X_1 \in [0, L], \ X_2 \in [0, H], \ X_3 \in [0, L]\}$$

with X_i the coordinates with respect to the axis $\mathbf{e}_i$, $i = 1, \ldots, 3$. The aspect ratio was chosen to be $L/H = 10$. As regards the boundary conditions, a displacement $u_3 = 1$ mm in the direction $\mathbf{e}_3$ is rapidly applied to the upper face (orthogonal to $\mathbf{e}_2$) and held for 2500 s, while the bottom face is clamped ($\mathbf{u} = \mathbf{0}$). All the other faces of the specimen are stress-free. The material parameters used for the simulations are those listed in Table 2, with the addition of $\tau_1 = 3000$ s, $\tau_2 = 1000$ s, $\tau_4 = 2000$ s, $\tau_3 = \tau_5 = 0$. Discretization is performed with 5012 tetrahedral elements, while degree 2 polynomials are used to approximate the displacement field $\mathbf{u}$ and degree 1 polynomials are used for the state variable $\mathbf{C}_v^{-1}$.

Results are shown in Figs. 5–6 in terms of the average Piola stress components, computed in the middle plane of the specimen, that is, we evaluate

$$\bar{S}_{32}(t) = \frac{1}{L^2} \int_{S_0} S_{32}(X, t) \, dX, \qquad \bar{S}_{22}(t) = \frac{1}{L^2} \int_{S_0} S_{22}(X, t) \, dX, \quad (5.55)$$
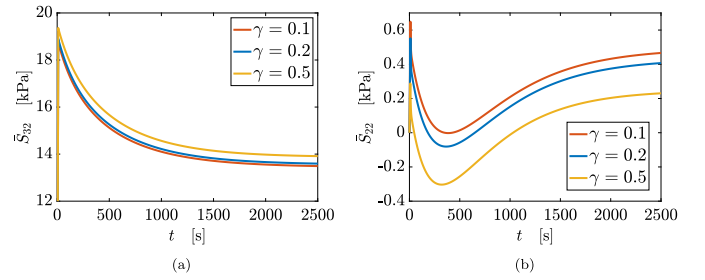

Fig. 6. Simple shear simulations for different relative stiffness of the fibres $\gamma = \gamma_{\mathrm{ov}}$ and fixed $\mathbf{A}_0 = \mathrm{diag}(0.1, 0.2, 0.7)$. (a): average stress $\bar{S}_{32}$. (b): average stress $\bar{S}_{22}$.

where

$$S_0 = \{(X_1, X_2, X_3) \mid X_1 \in [0, L], \ X_2 = H/2, \ X_3 \in [0, L]\} \, .$$

Specifically, Fig. 5 displays $\bar{S}_{32}$ and $\bar{S}_{22}$ over time for different initial fibre distributions $\mathbf{A}_0$. As expected, when the displacement is applied, the shear stress $\bar{S}_{32}$ relaxes to a value which increases as the fraction of fibres along the direction $\mathbf{e}_2$ is increased (see Fig. 5(a)). Interestingly, whilst the shear stress $\bar{S}_{32}$ exhibits a monotonically decreasing behaviour as expected from such a test, the normal stress $\bar{S}_{22}$ is non-monotonic and after an initial decrease it starts increasing again, until it reaches the steady state.

This effect is even more evident when investigating the material response for increasing stiffness of the reinforcing fibres, as done in Fig. 6 for fixed $\mathbf{A}_0 = \mathrm{diag}(0.1, 0.2, 0.7)$ and varying $\gamma = \gamma_{\mathrm{ov}}$. While the shear stress relaxes to a steady state value that increases with fibre stiffness, the stress $\bar{S}_{22}$ exhibits a non-monotonic behaviour, as evident from Fig. 6(b). In particular, if the fibres are sufficiently stiffer than the matrix, the stress is initially positive, indicating that the specimen would contract in absence of clamping force (negative Poynting effect), but then the stress changes sign, meaning that the specimen would start expanding (positive Poynting effect). Yet, at steady state, $\bar{S}_{22}$ takes a positive value. This time dependent behaviour of the Poynting effect was already discussed for isotropic viscoplastic materials in Califano and Ciambella (2023).

6. Conclusions

Soft biological materials exhibit complex anisotropic viscoelastic behaviour, arising from the inherent alignment of structural elements, such as fibres or collagen networks, which are often distributed statistically and require an appropriate treatment from both a theoretical and a computational viewpoint. In addition, a variety of material responses like stress relaxation, creep, and hysteresis, all with a directional dependence, emerges when viscoelastic reinforced tissues are tested experimentally to assess their mechanical properties.

Building upon previous works in nonlinear anisotropic viscoelasticity, we have developed a novel model that incorporates a distribution of fibres through a generalized orientation tensor approach, enabling us to capture the aforementioned material behaviours. The key elements of our work are as follows: (i) the deformation gradient is decomposed into multiplicative elastic and viscous components, where the latter influences the anisotropy and material symmetry of the body, which evolve over time; (ii) the elastic energy is separated into two components, one dependent on the strain relative to the reference state and the reference orientation tensor, and the other dependent on the strain relative to the remodelled state and on the orientation tensor modified by the viscous part of the deformation; (iii) a flow rule formulated in terms of referential variables is derived, governing the evolution of the viscous strain and featuring five characteristic time scales; (iv) the same flow rule is demonstrated to emerge as a minimization problem

for a proper Rayleighian functional using Onsager's variational principle, which is beneficial from a computational perspective. Finally, the implementation of the model into a finite element framework has been discussed, and the features of the model are shown through some benchmark problems in viscoelasticity.

There are still a number of interesting aspects that could be investigated in future works, such as the study of dispersion and waves, which was recently done for Kelvin–Voigt solids in Coco and Saccomandi (2023). Moreover, the promising referential approach adopted in the present paper also suggests to delve into a formulation of viscoelasticity in terms of the inverse viscous strain. Finally, applications of the proposed framework are foreseen in tissue mechanics, where the interplay between mechanical and biochemical factors is relevant. For instance, the consideration of active fibres would allow to study the material response to electro-chemical stimuli, which is an important aspect in the mechanics of reproductive tissues (Huntington et al., 2021).

CRediT authorship contribution statement

Jacopo Ciambella: Writing – review & editing, Writing – original draft, Supervision, Formal analysis, Conceptualization, Funding acquisition, Investigation, Methodology. **Giulio Lucci:** Writing – review & editing, Writing – original draft, Software, Investigation, Formal analysis, Conceptualization, Visualization. **Paola Nardinocchi:** Writing – review & editing, Writing – original draft, Supervision, Methodology, Formal analysis, Conceptualization, Funding acquisition, Investigation.

Declaration of competing interest

The authors declare that they have no known competing financial interests or personal relationships that could have appeared to influence the work reported in this paper.

Data availability

No data was used for the research described in the article.

Appendix. Supplementary calculations

Elastic invariants

As a consequence of structural frame indifference (SFI), the overstress elastic energy φ_{ov} is an isotropic function of the two tensors $\mathbf{C}_e$ and $\mathbf{A}_v$. Therefore, it can be expressed in terms of their invariants $I_1^e, \ldots, I_5^e$, as usually done for anisotropic materials, i.e.,

$$\varphi_{ov} = \varphi_{ov}(\mathbf{C}_e, \mathbf{A}_v) = \hat{\varphi}_{ov}(I_1^e, I_2^e, I_3^e, I_4^e, I_5^e). \tag{A.1}$$

Starting from their definitions, we firstly show that the invariants as well as their derivatives can indeed be expressed as functions of $\mathbf{C}$, $\mathbf{F}_v$, $\mathbf{C}_v$ and $\mathbf{A}_0$; such a result will allow us to express the right hand side of Eq. (3.26) as a function of $\mathbf{C}$, $\mathbf{C}_v$ and $\mathbf{A}_0$ only.

By using the common definitions of the invariants together with Eq. (2.4), we obtain

$$I_1^e := \mathbf{I} \cdot \mathbf{C}_e = \mathbf{C}_v^{-1} \cdot \mathbf{C}, \tag{A.2}$$

$$I_2^e := \mathbf{I} \cdot \mathbf{C}_e^* = \frac{1}{\det \mathbf{C}_v} \mathbf{C}_v \cdot \mathbf{C}^*, \tag{A.3}$$

$$I_3^e := \det \mathbf{C}_e = \frac{\det \mathbf{C}}{\det \mathbf{C}_v}, \tag{A.4}$$

$$I_4^e := \mathbf{A}_v \cdot \mathbf{C}_e = \frac{\mathbf{C} \cdot \mathbf{A}_0}{\mathbf{C}_v \cdot \mathbf{A}_0}, \tag{A.5}$$

$$I_5^e := \mathbf{A}_v \cdot \mathbf{C}_e^2 = \frac{\mathbf{C} \, \mathbf{C}_v^{-1} \mathbf{C} \cdot \mathbf{A}_0}{\mathbf{C}_v \cdot \mathbf{A}_0}, \tag{A.6}$$

with the derivatives with respect to $\mathbf{C}_e$ given by

$$\frac{\partial I_1^e}{\partial \mathbf{C}_e} = \mathbf{I}, \tag{A.7}$$

$$\frac{\partial I_2^e}{\partial \mathbf{C}_e} = (\mathbf{I} \cdot \mathbf{C}_e)\,\mathbf{I} - \mathbf{C}_e = (\mathbf{C}_v^{-1} \cdot \mathbf{C})\mathbf{I} - \mathbf{F}_v^{-T}\mathbf{C}\,\mathbf{F}_v^{-1}, \tag{A.8}$$

$$\frac{\partial I_3^e}{\partial \mathbf{C}_e} = \mathbf{C}_e^* = \frac{\det \mathbf{C}}{\det \mathbf{C}_v}\,\mathbf{F}_v\mathbf{C}^{-1}\mathbf{F}_v^T, \tag{A.9}$$

$$\frac{\partial I_4^e}{\partial \mathbf{C}_e} = \mathbf{A}_v = \frac{\mathbf{F}_v\,\mathbf{A}_0\,\mathbf{F}_v^T}{\mathbf{C}_v \cdot \mathbf{A}_0}, \tag{A.10}$$

$$\frac{\partial I_5^e}{\partial \mathbf{C}_e} = \mathbf{A}_v\mathbf{C}_e + \mathbf{C}_e\mathbf{A}_v = \frac{2}{\mathbf{C}_v \cdot \mathbf{A}_0}\,\mathrm{sym}\left(\mathbf{F}_v\,\mathbf{A}_0\,\mathbf{C}\,\mathbf{F}_v^{-1}\right), \tag{A.11}$$

as well as derivatives with respect to $\mathbf{A}_v$ given by

$$\frac{\partial I_4^e}{\partial \mathbf{A}_v} = \mathbf{C}_e = \mathbf{F}_v^{-T}\mathbf{C}\,\mathbf{F}_v^{-1}, \tag{A.12}$$

$$\frac{\partial I_5^e}{\partial \mathbf{A}_v} = \mathbf{C}_e^2 = \mathbf{F}_v^{-T}\mathbf{C}\,\mathbf{C}_v^{-1}\,\mathbf{C}\,\mathbf{F}_v^{-1}. \tag{A.13}$$

The Eshelby tensor

We now use (A.1)–(A.13) to rewrite the right-hand side of Eq. (3.26) by explicitly computing $\widetilde{\mathbf{E}}_{sh} := 2J_v\mathbf{F}_v^T\mathbf{E}_{sh}\mathbf{F}_v$. Specifically, by pulling back the three terms in Eq. (3.20) with $\mathbf{F}_v$, we obtain

$$\widetilde{\mathbf{E}}_1 := \mathbf{F}_v^T\,\mathrm{sym}\left(\mathbf{C}_e\frac{\partial\varphi_{ov}}{\partial\mathbf{C}_e}\right)\mathbf{F}_v = (\varphi_{ov})_{,1}\,\mathbf{C} + (\varphi_{ov})_{,2}\left((\mathbf{C}_v^{-1}\cdot\mathbf{C})\mathbf{C} - \mathbf{C}\mathbf{C}_v^{-1}\mathbf{C}\right)$$
$$+ (\varphi_{ov})_{,3}\frac{\det\mathbf{C}}{\det\mathbf{C}_v}\mathbf{C}_v + (\varphi_{ov})_{,4}\frac{\mathrm{sym}(\mathbf{C}\mathbf{A}_0\mathbf{C}_v)}{\mathbf{C}_v\cdot\mathbf{A}_0}$$
$$+ (\varphi_{ov})_{,5}\frac{\mathbf{C}\,\mathbf{A}_0\,\mathbf{C} + \mathrm{sym}(\mathbf{C}\,\mathbf{C}_v^{-1}\,\mathbf{C}\,\mathbf{A}_0\,\mathbf{C}_v)}{\mathbf{C}_v\cdot\mathbf{A}_0},$$

$$\widetilde{\mathbf{E}}_2 := \mathbf{F}_v^T\,\mathrm{sym}\left(\frac{\partial\varphi_{ov}}{\partial\mathbf{A}_v}\mathbf{A}_v\right)\mathbf{F}_v$$
$$= (\varphi_{ov})_{,4}\frac{\mathrm{sym}(\mathbf{C}\mathbf{A}_0\mathbf{C}_v)}{\mathbf{C}_v\cdot\mathbf{A}_0} + (\varphi_{ov})_{,5}\frac{\mathrm{sym}(\mathbf{C}\mathbf{C}_v^{-1}\mathbf{C}\mathbf{A}_0\mathbf{C}_v)}{\mathbf{C}_v\cdot\mathbf{A}_0},$$

$$\widetilde{\mathbf{E}}_3 := \mathbf{F}_v^T\left(\frac{\partial\varphi_{ov}}{\partial\mathbf{A}_v}\mathbf{A}_v\cdot\mathbf{I}\right)\mathbf{A}_v\mathbf{F}_v$$
$$= \left((\varphi_{ov})_{,4}\frac{\mathbf{C}\mathbf{A}_0\cdot\mathbf{I}}{\mathbf{C}_v\cdot\mathbf{A}_0} + (\varphi_{ov})_{,5}\frac{\mathbf{C}\mathbf{C}_v^{-1}\mathbf{C}\mathbf{A}_0\cdot\mathbf{I}}{\mathbf{C}_v\cdot\mathbf{A}_0}\right)\frac{\mathbf{C}_v\mathbf{A}_0\mathbf{C}_v}{\mathbf{C}_v\cdot\mathbf{A}_0},$$

such that the tensor $\widetilde{\mathbf{E}}_{sh}$ is

$$\widetilde{\mathbf{E}}_{sh} := 2J_v\mathbf{F}_v^T\mathbf{E}_{sh}\mathbf{F}_v = -4\varrho_0\widetilde{\mathbf{E}}_1 + 4\varrho_0\widetilde{\mathbf{E}}_2 - 4\varrho_0\widetilde{\mathbf{E}}_3$$
$$= -4\varrho_0\left[(\varphi_{ov})_{,1}\mathbf{I} + (\varphi_{ov})_{,2}(\mathbf{C}_v^{-1}\cdot\mathbf{C})\mathbf{I} - (\varphi_{ov})_{,2}\mathbf{C}\mathbf{C}_v^{-1}\right]\mathbf{C} - 4\varrho_0(\varphi_{ov})_{,3}\frac{\det\mathbf{C}}{\det\mathbf{C}_v}\mathbf{C}_v$$
$$-4\varrho_0(\varphi_{ov})_{,4}\frac{\mathbf{C}\cdot\mathbf{A}_0}{(\mathbf{C}_v\cdot\mathbf{A}_0)^2}\mathbf{C}_v\mathbf{A}_0\mathbf{C}_v$$
$$-4\varrho_0(\varphi_{ov})_{,5}\left[\frac{\mathbf{C}\mathbf{A}_0\mathbf{C}}{\mathbf{C}_v\cdot\mathbf{A}_0} + \frac{\mathbf{C}\mathbf{C}_v^{-1}\mathbf{C}\cdot\mathbf{A}_0}{(\mathbf{C}_v\cdot\mathbf{A}_0)^2}\mathbf{C}_v\mathbf{A}_0\mathbf{C}_v\right],$$

that is a function of $\mathbf{C}$, $\mathbf{C}_v$, and $\mathbf{A}_0$, and corresponds to minus the right-hand side of Eq. (4.33).

References

Alnæs, M., Blechta, J., Hake, J., Johansson, A., Kehlet, B., Logg, A., Richardson, C., Ring, J., Rognes, M.E., Wells, G.N., 2015. The FEniCS project version 1.5. Arch. Numer. Softw. 3 (100).

Ateshian, G.A., Rajan, V., Chahine, N.O., 2009. Finite element implementation of mechanochemical phenomena in neutral deformable porous media under finite deformation. J. Biomech. Eng. 131 (7), 071009.

Boote, C., Dennis, S., Meek, K.M., Quantock, A.J., 2006. Mapping collagen organization in the human cornea: left and right eyes are structurally distinct. Investig. Ophthalmol. Vis. Sci. 47 (3), 901–908.

Califano, F., Ciambella, J., 2023. Viscoplastic simple shear at finite strains. Proc. R. Soc. Lond. Ser. A Math. Phys. Eng. Sci. 479, 20230603.

Canham, P.B., Finlay, H.M., Dixon, J.G., 1989. Measurements of the mechanical properties of cerebral arteries and aneurysms. In: Cerebral Aneurysms: Advances in Diagnosis and Therapy. Springer, Boston, MA, pp. 29–40.

Ciambella, J., Lucci, G., Nardinocchi, P., Preziosi, L., 2022. Passive and active fiber reorientation in anisotropic materials. Internat. J. Engrg. Sci. 176, 103688.

Ciambella, J., Nardinocchi, P., 2019. Torque-induced reorientation in active fibre-reinforced materials. Soft Matter 15 (9), 2081–2091.

Ciambella, J., Nardinocchi, P., 2021. A structurally frame-indifferent model for anisotropic visco-hyperelastic materials. J. Mech. Phys. Solids 147, 104247.

Ciambella, J., Nardinocchi, P., 2022. Non-affine fiber reorientation in finite inelasticity. J. Elasticity 153, 735–753.

Clark-Patterson, G.L., Finlay, H.M., McGuire, J.A., Desrosiers, L., Knoepp, L.R., De Vita, R., Miller, K.S., 2021. Investigation of murine vaginal creep response to altered mechanical loads. J. Biomech. Eng. 143 (12), 121008.

Coco, M., Saccomandi, G., 2023. On the Kelvin–Voigt model in anisotropic viscoelasticity. Math. Mech. Solids 28 (12), 2581–2595.

Coleman, B.D., Noll, W., 1963. The thermodynamics of elastic materials with heat conduction and viscosity. Arch. Ration. Mech. Anal. 13 (1), 167–178.

DiCarlo, A., Quiligotti, S., 2002. Growth and balance. Mech. Res. Commun. 29 (6), 449–456.

Doi, M., 2011. Onsager's variational principle in soft matter. J. Phys.: Condens. Matter 23, 284118.

Doi, 2021. Onsager principle in polymer dynamics. Prog. Polym. Sci. 112, 101339.

Driessen, N.J., Bouten, C.V., Baaijens, F.P., 2005. A computational model for collagen fibre remodelling in the arterial wall. Comput. Methods Biomech. Biomed. Eng. 8 (5), 295–306.

Dubik, J., Tartaglione, A., Miller, K.S., Dillard, D.A., De Vita, R., 2022. History-dependent deformations of rat vaginas under inflation. Integr. Comp. Biol. 62, 625–640.

Ericksen, J.L., 1960. Transversely isotropic fluids. Kolloid-Zeitschrift (ISSN: 03686590) 173 (2), 117–122. http://dx.doi.org/10.1007/BF01502416.

Fancello, E., Ponthot, J.-P., Stainier, L., 2006. A variational formulation of constitutive models and updates in non-linear finite viscoelasticity. Internat. J. Numer. Methods Engrg. 65 (11), 1831–1864.

Finlay, H.M., Whittaker, P., Canham, P.B., 1998. Collagen organization in the branching region of human cerebral aneurysms. J. Vasc. Res. 35 (2), 77–84.

Freed, A.D., Einstein, D.R., Vesely, I., 2005. A new constitutive framework for arterial wall mechanics and a comparative study of material models. J. Biomech. 38 (3), 509–516.

Fung, Y.C., 1993. Biomechanics: Mechanical Properties of Living Tissues. Springer-Verlag.

Gasser, T.C., Ogden, R.W., Holzapfel, G.A., 2006. Hyperelastic modelling of arterial layers with distributed collagen fibre orientations. J. R. Soc. Interface 3, 15–35.

Gizzi, A., Pandolfi, A., Vasta, M., 2016a. Statistical characterization of the anisotropic strain energy in soft materials with distributed fibers. Mech. Mater. 92, 119–138.

Gizzi, A., Pandolfi, A., Vasta, M., 2016b. Viscoelectromechanics modeling of intestine wall hyperelasticity. Int. J. Comput. Methods Eng. Sci. Mech. 17 (3), 143–155.

Gotschi, T., Scharer, Y., Gennison, J.-L., Snedeker, J.G., 2023. Investigation of the relationship between tensile viscoelasticity and unloaded ultrasound shear wave measurements in ex vivo tendon. J. Biomech. 146, 111411.

Green, A.E., Naghdi, P.M., 1971. Some remarks on elastic-plastic deformation at finite strain. Internat. J. Engrg. Sci. 9 (12), 1219–1229.

Grillo, A., Wittum, G., Tomic, A., Federico, S., 2014. Remodelling in statistically oriented fibre-reinforced materials and biological tissues. Math. Mech. Solids 20, 1107–1129.

Gurtin, M.E., Fried, E., Anand, L., 2013. The Mechanics and Thermodynamics of Continua. Cambridge University Press.

Hashlamoun, K., Grillo, A., Federico, S., 2016. Efficient evaluation of the material response of tissues reinforced by statistically oriented fibres. Z. Angew. Math. Phys. 67, 113.

Huntington, A., Abramowitch, S., Moalli, P., De Vita, R., 2021. Strains induced in the vagina by smooth muscle contractions. Acta Biomater. 129, 178–187.

Komai, Y., Ushiki, T., 1991. The three-dimensional organization of collagen fibrils in the human cornea and sclera. Investig. Ophthalmol. Vis. Sci. 32 (8), 2244–2258.

Kumar, A., Lopez-Pamies, O., 2016. On the two-potential constitutive modeling of rubber viscoelastic materials. C. R. Méc. 344, 102–112.

Lanir, Y., 1979. A structural theory for the homogeneous biaxial stress-strain relationships in flat collagenous tissues. J. Biomech. 12 (6), 423–436.

Lanir, Y., 2017. Multi-scale structural modeling of soft tissues mechanics and mechanobiology. J. Elasticity 129 (1–2), 7–48.

Latorre, M., Montáns, F.J., 2015. Anisotropic finite strain viscoelasticity based on the Sidoroff multiplicative decomposition and logarithmic strains. Comput. Mech. 56 (3), 503–531.

Latorre, M., Montáns, F.J., 2016. Fully anisotropic finite strain viscoelasticity based on a reverse multiplicative decomposition and logarithmic strains. Comput. Struct. 163, 56–70.

Lee, E.H., 1969. Elastic-plastic deformation at finite strains. J. Appl. Mech. 36 (1), 1–6.

Liu, H., Holzapfel, G.A., Skallerud, B.H., Prot, V., 2019. Anisotropic finite strain viscoelasticity: Constitutive modeling and finite element implementation. J. Mech. Phys. Solids 124, 172–188.

Logg, A., Wells, G.N., Hake, J., 2012. DOLFIN: A C++/Python finite element library. In: Automated Solution of Differential Equations by the Finite Element Method. Springer, pp. 173–225.

Miehe, C., Lambrecht, M., Gürses, E., 2004. Analysis of material instabilities in inelastic solids by incremental energy minimization and relaxation methods: evolving deformation microstructures in finite plasticity. J. Mech. Phys. Solids 52, 2725–2769.

Mierke, C.T., 2022. Viscoelasticity, like forces, plays a role in mechanotransduction. Front. Cell Dev. Biol. 10, 1–58.

Ortiz, M., Stainier, L., 1999. The variational formulation of viscoplastic constitutive updates. Comput. Methods Appl. Mech. Engrg. 171, 419–444.

Pandolfi, A., Gizzi, A., Vasta, M., 2016. Coupled electro-mechanicalmodelsof fiber-distributedactivetissues. J. Biomech. 49, 2436–2444.

Pandolfi, A., Gizzi, A., Vasta, M., 2017. Visco-electro-elastic models of fiber-distributed active tissues. Meccanica 52, 3399–3415.

Pandolfi, A., Vasta, M., 2012a. A structural model for the viscoelastic behavior of arterial walls: Continuum formulation and finite element analysis. J. Biomech. 45 (4), 720–732.

Pandolfi, A., Vasta, M., 2012b. Fiber distributed hyperelastic modeling of biological tissues. Mech. Mater. 44, 151–162.

Reese, S., Govindjee, S., 1998. A theory of finite viscoelasticity and numerical aspects. Int. J. Solids Struct. 35 (26–27), 3455–3480.

Sacks, M.S., 2003. A method for planar biaxial mechanical testing that includes in-plane shear. J. Biomech. Eng. 125 (1), 54–60.

Sadik, S., Yavari, A., 2024. Nonlinear anisotropic viscoelasticity. J. Mech. Phys. Solids 182, 105461.

Schriefl, A.J., Zeindlinger, G., Pierce, D.M., Regitnig, P., Holzapfel, G.A., 2011. Determination of the layer-specific distributed collagen fibre orientations in human thoracic and abdominal aortas and common iliac arteries. J. R. Soc. Interface 8 (55), 1462–1471.

Spencer, A.J.M., 2004. Some results in the theory of non-Newtonian transversely isotropic fluids. J. Non-Newton. Fluid Mech. 112, 83–90.

Teichtmeister, S., Holzapfel, G.A., 2022. A constitutive model for fibrous tissues with cross-linked collagen fibers including dispersion — With an analysis of the poynting effect. J. Mech. Phys. Solids 164, 104911.

Upadhyay, K., Subhash, G., Spearot, D., 2020. Visco-hyperelastic constitutive modeling of strain rate sensitive soft materials. J. Mech. Phys. Solids 135, 103777.

Verron, E., 2015. A review on finite element simulation of the human meniscus. Biomech. Model. Mechanobiol. 14 (4), 761–771.

Vianello, M., 1996. Optimization of the stored energy and coaxiality of strain and stress in finite elasticity. J. Elasticity 44, 193–202.

Wollner, M.P., Terzano, M., Rolf-Pissarczyk, M., Holzapfel, G.A., 2023. A general model for anisotropic pseudo-elasticity and viscoelasticity at finite strains. J. Mech. Phys. Solids 180, 105403.